

# Transitions in eigenvalue and wavefunction structure in (1+2)-body random matrix ensembles with spin

Manan Vyas,<sup>1</sup> V. K. B. Kota,<sup>1,2,\*</sup> and N. D. Chavda<sup>3</sup><sup>1</sup>*Physical Research Laboratory, Ahmedabad 380 009, India*<sup>2</sup>*Department of Physics, Laurentian University, Sudbury, Ontario, Canada P3E 2C6*<sup>3</sup>*Applied Physics Department, Faculty of Technology and Engineering, M.S. University of Baroda, Vadodara 390 001, India*

(Received 29 September 2009; revised manuscript received 15 December 2009; published 12 March 2010)

Finite interacting Fermi systems with a mean-field and a chaos generating two-body interaction are modeled by one plus two-body embedded Gaussian orthogonal ensemble of random matrices with spin degree of freedom [called EGOE(1+2)-s]. Numerical calculations are used to demonstrate that, as  $\lambda$ , the strength of the interaction (measured in the units of the average spacing of the single-particle levels defining the mean-field), increases, generically there is Poisson to GOE transition in level fluctuations, Breit-Wigner to Gaussian transition in strength functions (also called local density of states) and also a duality region where information entropy will be the same in both the mean-field and interaction defined basis. Spin dependence of the transition points  $\lambda_c$ ,  $\lambda_F$ , and  $\lambda_d$ , respectively, is described using the propagator for the spectral variances and the formula for the propagator is derived. We further establish that the duality region corresponds to a region of thermalization. For this purpose we compared the single-particle entropy defined by the occupancies of the single-particle orbitals with thermodynamic entropy and information entropy for various  $\lambda$  values and they are very close to each other at  $\lambda = \lambda_d$ .

DOI: [10.1103/PhysRevE.81.036212](https://doi.org/10.1103/PhysRevE.81.036212)

PACS number(s): 05.45.Mt, 05.30.-d, 74.78.Na, 24.60.Lz

## I. INTRODUCTION

Finite quantum systems such as nuclei, atoms, quantum dots, and small metallic grains share one common property: their constituents interact via two-particle interactions. However, the classical Gaussian orthogonal ensemble (GOE) of random matrices (similarly the unitary ensemble GUE or the symplectic ensemble GSE) is an ensemble of multibody not two-body interactions; GOE representation of the Hamiltonian ( $H$ ) for a  $m$  particle system implies  $m$ -body forces. Therefore, a better random matrix hypotheses for finite quantum systems is to consider the effective interactions to be random. Matrix ensembles generated by random two-body interactions, called two-body ensembles, model what one may call many-body chaos or stochasticity exhibited by these systems. These ensembles are defined by representing the two-particle Hamiltonian by one of the classical ensembles (GOE or GUE or GSE) and then the  $m > 2$  particle  $H$  matrix is generated by the  $m$  particle Hilbert-space geometry [1,2]. The key element here is the recognition that there is a Lie algebra that transports the information in the two-particle spaces to many-particle spaces [2,3]. Thus the random matrix ensemble in the two particle spaces is embedded in the  $m$  particle  $H$  matrix and therefore these ensembles are more generically called embedded ensembles (EEs) [2,4]. Random two-body interactions were introduced first in nuclear physics in 1970–1971 [1]. Nuclear shell-model calculations showed differences between these ensembles and GOE both in one-point (density of states) and two-point (fluctuations) functions [2,4,5]. Simplest of these ensembles is the embedded Gaussian orthogonal ensemble generated by

two-body interactions for spinless fermion systems [called EGOE(2)] [2]. The GUE and GSE versions as well as the ensembles for boson systems are not considered in this paper. Note that just as the EGOE(2) ensemble, it is possible to define  $k$ -body ( $k < m$ ) ensembles EGOE( $k$ ). Some of the generic results, derived numerically and analytically, for EGOE( $k$ ) are as follows: (i) state densities approach Gaussian form for large  $m$  and they exhibit, as  $m$  increases from  $k$ , semicircle to Gaussian transition with  $m=2k$  being the transition point [4,6]; (ii) fluctuations follow GOE (as far as one can infer from numerical examples) [4]; (iii) there is average fluctuation separation with increasing  $m$  and the averages are determined by a few long-wavelength modes in the normal-mode decomposition of the density of states [2,4,7]; (iv) smoothed (ensemble averaged) transition strength densities take bivariate Gaussian form and as a consequence transition strength sums originating from a given eigenstate will be close to a ratio of two Gaussians [8]; and (v) cross correlations between spectra with different particle numbers will be nonzero [9,10]. For reviews on EGOE see [4,11,12]. Besides the two-body interaction, Hamiltonians for realistic systems also contain a mean-field one-body part (generating shell structure) and therefore a more appropriate random matrix ensemble for finite quantum systems is EGOE(1+2), the embedded GOE of one plus two-body interactions [12–14]. This ensemble contains a parameter  $\lambda$ , the strength of the interaction measured in the units of the average spacing of the single-particle (sp) states. As the value of  $\lambda$  increases from zero, level fluctuations exhibit transition from Poisson to GOE at  $\lambda = \lambda_c$  [15]. With further increase in the  $\lambda$  value, strength functions (also called local density of states) make a transition from Breit-Wigner (BW) to Gaussian form at  $\lambda = \lambda_F \gg \lambda_c$  [16–18]. Beyond this point, there is a region around  $\lambda = \lambda_d$  where some statistics become same in the eigenbasis of the mean-field Hamiltonian and the pure two-

\*Corresponding author.

FAX: +91-79-26314460; vkbkota@prl.res.in

body Hamiltonian [19,20] (though not yet proved, this result perhaps extends to any basis [21]). Equivalently, all different definitions for thermodynamic properties such as entropy and temperature coincide at  $\lambda = \lambda_d$ . Besides these, generic properties of EGOE(2) are valid for EGOE(1+2) in the strong-coupling limit, i.e., for  $\lambda \gg \lambda_F$ . For a detailed discussion of the three chaos markers ( $\lambda_c, \lambda_F, \lambda_d$ ) generated by EGOE(1+2) and also for applications of the ensemble see [12,21–23] and references therein.

Eigenstates of realistic systems carry, besides the particle number, additional quantum numbers. For example, the spin ( $S$ ) quantum number is important for quantum dots and metallic grains. Similarly for atomic nuclei, important are the orbital angular momentum ( $L$ ), spin ( $S$ ) and isospin ( $T$ ), i.e.,  $LST$  or the total angular momentum  $J$  ( $\vec{J} = \vec{L} + \vec{S}$ ) and isospin, i.e.,  $JT$  or in some situations just  $J$  [5,24]. As group symmetries define various quantum numbers, in general one has to consider EE with group symmetries [10,25]. Numerical as well analytical study of these more general ensembles is challenging due to the complexities of group theory and also due to large matrix dimensions for  $m \geq 10$ . The first non-trivial but at the same time important (from the point of view of its applications) embedded ensembles are EE(2)-s and EE(1+2)-s with spin degree of freedom, for a system of interacting fermions. In the last decade, the GOE version, the embedded Gaussian orthogonal ensemble of one plus two-body interactions with spin degree of freedom [EGOE(1+2)-s], has received considerable attention. Both numerical [26,27] and analytical [25,28,29] methods for analyzing and applying this ensemble have been developed. Using these, several results are obtained and briefly they are as follows: (i) fixed- $(m, S)$  density of levels is established, using numerical results, to be Gaussian [26,28,30]; (ii) lower order cross correlations in spectra with different  $(m, S)$  are studied both numerically and analytically and they are found to be larger compared to those for the spinless fermion systems [10,26]; (iii) ground-state spin structure investigated using second and fourth moments established that with random interactions there is preponderance of  $S=0$  ground states [25,28]; (iv) delay in Stoner instability in itinerant magnetic systems due to random interactions has been established and thus with random interactions much stronger exchange interaction is needed for ground-state magnetization in irregular quantum dots [30]; (v) it is shown that the odd-even staggering in the ground-state energies of nm-scale metallic grains, attributed normally due to mean-field orbital energy effects or coherent pairing effects, can also come from purely random two-body Hamiltonians [25,31]; (vi) expectation values of the pairing Hamiltonian in the eigenstates generated by random interactions showed that random interactions, even in the chaotic domain, exhibit strong pairing correlations in the ground-state region and they decrease as we go up in energy [29]; and (vii) random interactions with pairing and exchange interactions are shown to generate bimodal form for conductance peak spacing distributions in small metallic grains consistent with the results from microscopic calculations [29,32]. Thus, although the ground-state structures generated by EGOE(1+2)-s and also some results in the strong-coupling region have been investigated in some detail, the important question of chaos or transition markers generated

by the ensemble hasn't yet been investigated in any detail. It should be stressed that the chaos markers form the basis [21] for statistical spectroscopy [12,33–36] and also the BW to Gaussian transition plays an important role in characterizing multipartite entanglement and fidelity decay relevant for quantum information science (QIS) [23,37,38]. Our purpose in this paper is to establish that the EGOE(1+2)-s ensemble exhibits three chaos markers just as the EGOE(1+2) for spinless fermion systems and more importantly, by deriving the exact formula for the propagator of the spectral variances, the spin dependence of the markers is explained. These results, derived for the first time using an ensemble with additional symmetry (besides particle number), provide much stronger basis for statistical (nuclear and atomic) spectroscopy. In addition, as recognized only recently, entanglement and strength functions essentially capture the same information about eigenvector structure and therefore the change in the form ( $\delta$ -function to BW to Gaussian) of the strength functions in different regimes defined by the chaos markers determines entanglement properties in multiqubit systems [23,37–39]. Similarly, the chaos marker  $\lambda_d$  discussed ahead allows us to define a region of thermalization in finite interacting quantum systems modeled by EGOE and thermalization in generic isolated quantum systems has applications in QIS as emphasized in some recent papers [40–43]. Now we will give a preview.

In Sec. II, for completeness, some general aspects of EGOE(1+2)-s are discussed. In Sec. III analytical formula for the ensemble averaged spectral variance of fixed- $(m, S)$  eigenvalue densities is given and this plays a vital role in explaining the results presented in the remaining part of the paper. Some results for the excess parameter are discussed in Appendix A. Section IV gives the results for Poisson (in our calculations it is strictly not a Poisson) to GOE transition in level fluctuations. Section V gives the results for BW to Gaussian transition in strength functions. Section VI deals with the duality marker using information entropy. In Sec. VII, occupancies of sp orbitals and the corresponding sp entropy are considered and it is established that the duality region corresponds to a region of thermalization for the finite quantum system considered. Finally Sec. VIII gives some concluding remarks.

## II. EGOE(1+2)-s ENSEMBLE: PRELIMINARIES

Let us begin with a system of  $m$  ( $m > 2$ ) fermions distributed say in  $\Omega$  number of sp orbitals each with spin  $s = \frac{1}{2}$  so that the number of sp states  $N = 2\Omega$ . The sp states are denoted by  $|i, m_s = \pm \frac{1}{2}\rangle$  with  $i = 1, 2, \dots, \Omega$  and similarly the two particle antisymmetric states are denoted by  $|(ij)s, m_s\rangle_a$  with  $s = 0$  or 1. For one plus two-body Hamiltonians preserving  $m$  particle spin  $S$ , the one-body Hamiltonian is  $\hat{h}(1) = \sum_{i=1,2,\dots,\Omega} \epsilon_i n_i$ . Here the orbitals  $i$  are doubly degenerate,  $n_i$  are number operators and  $\epsilon_i$  are sp energies [it is in principle possible to consider  $\hat{h}(1)$  with off-diagonal energies  $\epsilon_{ij}$ ]. Similarly the two-body Hamiltonian  $\hat{V}(2)$  is defined by the two-body matrix elements  $\lambda_s V_{ijkl}^s = {}_a \langle (kl)s, m_s | \hat{V}(2) | (ij)s, m_s \rangle_a$  with the two-particle spins  $s = 0$

and 1. These matrix elements are independent of the  $m_s$  quantum number. Note that the  $\lambda_s$  are constants and for  $s=1$ , only  $i \neq j$  and  $k \neq l$  matrix elements exist. Thus  $\hat{V}(2) = \lambda_0 \hat{V}^{s=0}(2) + \lambda_1 \hat{V}^{s=1}(2)$  and the  $V$  matrix in two particle spaces is a direct sum matrix with the  $s=0$  and  $s=1$  space matrices having dimensions  $\Omega(\Omega+1)/2$  and  $\Omega(\Omega-1)/2$ , respectively. Now, EGOE(2)-s for a given  $(m, S)$  system is generated by defining the two parts of the two-body Hamiltonian to be independent GOE's [one for  $\hat{V}^{s=0}(2)$  and other for  $\hat{V}^{s=1}(2)$ ] in 2-particle spaces and then propagating the  $V(2)$  ensemble  $\{\hat{V}(2)\} = \lambda_0 \{\hat{V}^{s=0}(2)\} + \lambda_1 \{\hat{V}^{s=1}(2)\}$  to the  $m$ -particle spaces with a given spin  $S$  by using the geometry (direct product structure), defined by  $U(2\Omega) \supset U(\Omega) \otimes SU(2)$  algebra, of the  $m$ -particle spaces; here  $\{\}$  denotes ensemble. Then EGOE(1+2)-s is defined by the operator

$$\{\hat{H}\}_{\text{EGOE}(1+2)\text{-s}} = \hat{h}(1) + \lambda_0 \{\hat{V}^{s=0}(2)\} + \lambda_1 \{\hat{V}^{s=1}(2)\}, \quad (1)$$

where  $\{\hat{V}^{s=0}(2)\}$  and  $\{\hat{V}^{s=1}(2)\}$  in two particle spaces are GOE(1) and  $\lambda_0$  and  $\lambda_1$  are the strengths of the  $s=0$  and  $s=1$  parts of  $\hat{V}(2)$ , respectively. Note that GOE( $v^2$ ) means GOE with variance  $v^2$  for the off-diagonal matrix elements and  $2v^2$  for the diagonal matrix elements. From now onwards we drop the ‘‘hat’’ symbol over  $H$ ,  $h$  and  $V$  operators when there is no confusion.

The mean-field one-body Hamiltonian  $h(1)$  in Eq. (1) is a fixed one-body operator defined by the sp energies  $\epsilon_i$  with average spacing  $\Delta$  (it is possible to draw the  $\epsilon_i$ 's from the eigenvalues of a random ensemble [30] or from the center of a GOE [44]). Without loss of generality we put  $\Delta=1$  so that  $\lambda_0$  and  $\lambda_1$  are in the units of  $\Delta$ . Thus, EGOE(1+2)-s in Eq. (1) is defined by the five parameters  $(\Omega, m, S, \lambda_0, \lambda_1)$ . The action of the Hamiltonian operator defined by Eq. (1) on an appropriately chosen fixed- $(m, S)$  basis states generates the EGOE(1+2)-s ensemble in  $(m, S)$  spaces. The  $H$  matrix dimension  $d(m, S)$  for a given  $(m, S)$ , i.e., number of levels in the  $(m, S)$  space [with each of them being  $(2S+1)$ -fold degenerate], is

$$d(m, S) = \frac{(2S+1)}{(\Omega+1)} \binom{\Omega+1}{m/2+S+1} \binom{\Omega+1}{m/2-S}, \quad (2)$$

satisfying the sum rule  $\sum_S (2S+1) d(m, S) = \binom{N}{m}$ . For example for  $\Omega=m=8$ , the dimensions are 1764, 2352, 720, 63, and 1 for  $S=0, 1, 2, 3$ , and 4, respectively. Similarly for  $\Omega=m=10$ , the dimensions are 19 404, 29 700, 12 375, 1925, 99, and 1 for  $S=0-5$  and for  $\Omega=m=12$ , they are 22 6512, 38 2239, 19 6625, 44 044, 4214, 143, and 1 for  $S=0-6$ . It is useful to note that for the EGOE(1+2)-s ensemble three group structures are relevant and they are  $U(\Omega) \otimes SU(2)$ ,  $\sum_{S=0,1} O(N_{2,S}) \oplus$  and  $\sum_S O(N_{m,S}) \oplus$ ,  $m > 2$ . Here  $N_{m,S} = d(m, S)$ , the symbol  $\oplus$  stands for direct sum and  $O(r)$  is the orthogonal group in  $r$  dimensions. The  $U(\Omega) \otimes SU(2)$  algebra defines the embedding. The EGOE(2) ensemble has orthogonal invariance with respect to the  $\sum_{S=0,1} O(N_{2,S}) \oplus$  group acting in two particle spaces. However it is not invariant under the  $\sum_S O(N_{m,S}) \oplus$  group for  $m > 2$ . This group is appropriate if GOE representation for fixed- $(m, S)$   $H$  matrices is

employed; i.e., there is an independent GOE for each  $(m, S)$  subspace.

Given the sp energies  $\epsilon_i$  and the two-body matrix elements  $V_{ijkl}^s$ , the many particle Hamiltonian matrix for a given  $(m, S)$  can be constructed either using the  $M_S$  representation and a spin ( $S$ ) projection operator [26] or directly in a good  $S$  basis using angular-momentum algebra [27]. The former is equivalent to employing the algebra  $U(2\Omega) \supset U(\Omega) \oplus U(\Omega)$  and the latter corresponds to  $U(2\Omega) \supset U(\Omega) \otimes SU(2)$ . Just as in our earlier papers [26,29], we have employed the  $M_S$  representation for constructing the  $H$  matrices and the  $\hat{S}^2$  operator for projecting states with good  $S$ . Then the dimension of the basis space is  $\mathcal{D}(M_S^{min}) = \sum_S d(m, S)$ ;  $M_S^{min} = 0$  for  $m$  even and  $1/2$  for  $m$  odd. For example, for  $\Omega_S = m = 8$  we have  $\mathcal{D}(M_S^{min}) = 4900$ , for  $\Omega = 8$ ,  $m = 6$ ,  $\mathcal{D}(M_S^{min}) = 3136$  and for  $\Omega = m = 10$  we have  $\mathcal{D}(M_S^{min}) = 63\,404$ . It is important to note that here the construction of the  $m$  particle  $H$  matrix reduces to the problem of EGOE(1+2) for spinless fermion systems and hence Eqs. (1)–(3) of [12] will apply. From the dimensions given above, it is clear that numerical calculations will be prohibitive for  $m \geq 10$  even on best available computers. Therefore, most of the numerical investigations are restricted to  $m \leq 8$ . For properties related to a few lowest eigenvalues it is possible to go beyond  $m=8$  [31]. Now, before presenting the results for the three chaos markers generated by EGOE(1+2)-s, we will consider the ensemble averaged fixed- $(m, S)$  density of levels and present the exact formula for its variance.

### III. GAUSSIAN LEVEL DENSITIES AND ENSEMBLE AVERAGED SPECTRAL VARIANCES

#### A. Gaussian form for fixed- $(m, S)$ eigenvalue densities

Using the method discussed in Sec. II, we have numerically constructed the  $H$  matrix in large number of examples and by diagonalizing them obtained the ensemble averaged eigenvalue (level) densities  $\rho^{m,S}(E) = \langle \delta(H-E) \rangle^{m,S}$ . Note that the trace of an operator  $\mathcal{O}$  over a fixed- $(m, S)$  space is defined by  $\langle \langle \mathcal{O} \rangle \rangle^{m,S} = (2S+1)^{-1} \sum_{\alpha} \langle m, S, \alpha | \mathcal{O} | m, S, \alpha \rangle$  and similarly  $(m, S)$  space average is  $\langle \mathcal{O} \rangle^{m,S} = [(2S+1)d(m, S)]^{-1} \sum_{\alpha} \langle m, S, \alpha | \mathcal{O} | m, S, \alpha \rangle$ . From now onwards, we drop the ‘bar’ over  $\rho$  when there is no confusion. Results are shown for  $\Omega=8$  and  $m=6$  with  $S=0$  and 1 and  $\lambda_0 = \lambda_1 = \lambda = 0.3$  in Fig. 1. In these calculations and also for all other calculations reported in this paper we have chosen the sp energies to be  $\epsilon_i = i + 1/i$  with  $i = 1, 2, \dots, \Omega$  just as in many of the earlier papers [13,20,26,29]. Note that the second term ( $1/i$ ) in  $\epsilon_i$  has been added, as discussed first in [13], to avoid the degeneracy of many-particle states. To construct the eigenvalue density, we first make the centroids  $E_c(m, S)$  of all the members of the ensemble to be zero and variance  $\sigma^2(m, S)$  to be unity i.e., for each member we change the eigenvalues  $E$  to the standardized variables  $\hat{E} = [E - E_c(m, S)] / \sigma(m, S)$ . Note that the parameters  $E_c(m, S)$  and  $\sigma^2(m, S)$  depend also on  $\Omega$ . But for convenience, we will drop  $\Omega$  in  $E_c(m, S)$  and  $\sigma^2(m, S)$  throughout this paper. Then, using a bin size  $\Delta \hat{E} = 0.2$ , histograms for  $\rho^{m,S}(E)$  are generated. The calculated results are compared with both the

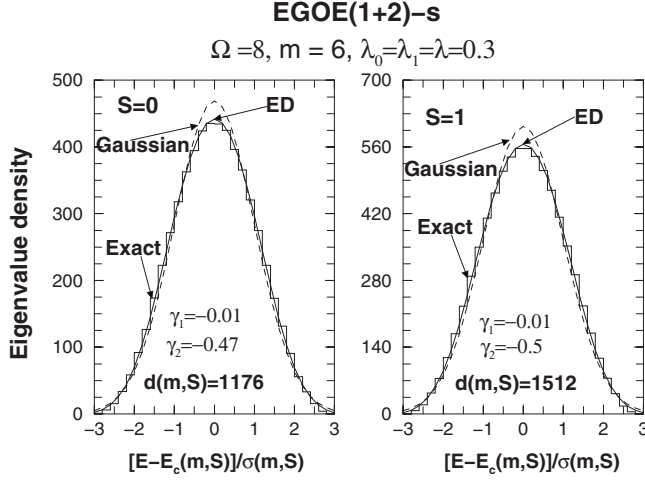


FIG. 1. Ensemble averaged eigenvalue density for a 20 member EGOE(1+2)-s ensemble with  $\Omega=8$ ,  $m=6$  and spins  $S=0$  and 1. The dashed curves give Gaussian representation and the continuous curves give Edgeworth corrected Gaussians [ $\rho_{ED}$  in Eq. (3)]. Values of the skewness and excess parameters are also given in the figure. In the plots, the densities for a given spin are normalized to the dimension  $d(m,S)$ . Note that the  $E_c(m,S)$  and  $\sigma(m,S)$  are fixed- $(m,S)$  energy centroids and spectral widths, respectively, of the eigenvalue densities. See text for further details.

Gaussian ( $\rho_G$ ) and Edgeworth (ED) corrected Gaussian ( $\rho_{ED}$ ) [45],

$$\rho_G(\hat{E}) = \frac{1}{\sqrt{2\pi}} \exp\left(-\frac{\hat{E}^2}{2}\right),$$

$$\rho_{ED}(\hat{E}) = \rho_G(\hat{E}) \left\{ 1 + \left[ \frac{\gamma_1}{6} \text{He}_3(\hat{E}) \right] + \left[ \frac{\gamma_2}{24} \text{He}_4(\hat{E}) + \frac{\gamma_1^2}{72} \text{He}_6(\hat{E}) \right] \right\}. \quad (3)$$

Here  $\gamma_1$  is the skewness and  $\gamma_2$  is the excess parameter. Similarly, He are the Hermite polynomials:  $\text{He}_3(x) = x^3 - 3x$ ,  $\text{He}_4(x) = x^4 - 6x^2 + 3$  and  $\text{He}_6(x) = x^6 - 15x^4 + 45x^2 - 15$ . From the results in Fig. 1, it is seen that the agreement between the exact and ED corrected Gaussians is excellent. Further numerical examples are given in [26,30] up to  $m=8$ . It has been well established that the ensemble averaged eigenvalue density takes Gaussian form in the case of spinless fermion as well as boson systems [2,6,12,46]. Combining these with the numerical results for the fixed- $(m,S)$  level densities, it can be concluded that the Gaussian form is generic for the embedded ensembles extending to those with good quantum numbers. This is further substantiated by the analytical results for the ensemble averaged  $\gamma_2(m,S)$  as discussed in Appendix A. We will present the analytical formula for the ensemble averaged spectral variances  $\overline{\sigma^2(m,S)}$ , i.e., for the variance of  $\rho^{m,S}(E)$  in Sec. III B.

It is important to point out that the variances  $\overline{\sigma^2(m,S)}$  propagate in a simple manner [47,48] from the corresponding three defining space variances, the variance in one-particle space  $\sigma^2(1, \frac{1}{2})$  and the two two-particle variances

$\overline{\sigma^2(2,s)} = \lambda_s^2 [d(2,s) + 1]$ ,  $s=0,1$ . Thus the  $(m,S)$  space variances are a linear combination of these three basic variances with the multiplying factors being simple functions of  $(\Omega, m, S)$ . These functions are called variance propagators as they carry the variance information from the defining space to the final  $(m,S)$  spaces and it is easy to derive formulas for them as given in Sec. III B. For example, the variances generated by the two-body part of the Hamiltonian for  $\lambda_0^2 = \lambda_1^2 = \lambda^2$  are of the form  $\overline{\sigma_{V(2)}^2(m,S)} = \lambda^2 P(\Omega, m, S)$ . The variance propagator  $P(\Omega, m, S)$ , given by Eq. (13) ahead, determines much of the behavior of the transitions in eigenvalue and wavefunction structure as discussed ahead.

### B. Propagation formulas for ensemble averaged spectral variances

Let us start with the fixed- $(m,S)$  energy centroids  $E_c(m,S) = \langle H \rangle^{m,S}$  for a one plus two-body Hamiltonian  $H = h(1) + V(2) = h(1) + [\lambda_0 V^{s=0}(2) + \lambda_1 V^{s=1}(2)]$ . The operator generating  $\langle H \rangle^{m,S}$  will be a polynomial, in the scalar operators  $\hat{n}$  and  $\hat{S}^2$ , of maximum body rank 2. A two-body operator is said to be of body rank 2, a three-body operator of body rank 3 and so on [2]. Note that  $\hat{n}$  is a one-body operator and  $\hat{S}^2$  is a one plus two-body operator. Hence only  $\hat{n}$ ,  $\hat{n}^2$  and  $\hat{S}^2$  are operators of maximum body rank 2 (for example, the operator  $\hat{n}\hat{S}^2$  is of maximum body rank 3). Then,  $E_c(m,S) = a_0 + a_1 m + a_2 m^2 + a_3 S(S+1)$ . Solving for the  $a_i$ 's in terms of  $E_c$  for  $m \leq 2$ , we obtain the well-known propagation formula for the energy centroids [47],

$$E_c(m,S) = [\langle h(1) \rangle^{1,1/2}] m + \lambda_0 \langle \langle V^{s=0}(2) \rangle \rangle^{2,0} \frac{P^0(m,S)}{4\Omega(\Omega+1)}$$

$$+ \lambda_1 \langle \langle V^{s=1}(2) \rangle \rangle^{2,1} \frac{P^1(m,S)}{4\Omega(\Omega-1)};$$

$$P^0(m,S) = [m(m+2) - 4S(S+1)],$$

$$P^1(m,S) = [3m(m-2) + 4S(S+1)],$$

$$\langle h(1) \rangle^{1,1/2} = \Omega^{-1} \sum_{i=1}^{\Omega} \epsilon_i,$$

$$\langle \langle V^{s=0}(2) \rangle \rangle^{2,0} = \sum_{i \leq j} V_{ijij}^{s=0}, \quad \langle \langle V^{s=1}(2) \rangle \rangle^{2,1} = \sum_{i < j} V_{ijij}^{s=1}. \quad (4)$$

Trivially the ensemble average of  $E_c$  from the  $V(2)$  part will be zero. However the covariances in the energy centroids generated by the two-body part  $H(2) = V(2)$  of  $H$  are nonzero,

$$\overline{\langle H(2) \rangle^{m,S} \langle H(2) \rangle^{m',S'}} = \frac{\lambda_0^2}{16\Omega(\Omega+1)} P^0(m,S) P^0(m',S') + \frac{\lambda_1^2}{16\Omega(\Omega-1)} P^1(m,S) P^1(m',S'). \quad (5)$$

The spectral variances  $\sigma^2(m,S) = \langle H^2 \rangle^{m,S} - [\langle H \rangle^{m,S}]^2$  are generated by an operator that is a polynomial, in the scalar

operators  $\hat{n}$  and  $\hat{S}^2$ , of maximum body rank 4. This gives  $\sigma^2(m, S) = \sum_{p=0}^4 a_p m^p + \sum_{q=0}^2 b_q m^q S(S+1) + c_0 [S(S+1)]^2$ . The nine parameters  $(a_i, b_i, c_i)$  can be written in terms of  $\epsilon_i$  and the two-body matrix elements  $V_{ijkl}^{s=0,1}$  using the embedding algebra  $U(N) \supset U(\Omega) \otimes SU(2)$ . The final result is given by Eq. (8) of [26] (this is derived using the results in [49]). We have carried out the ensemble average of  $\sigma_H^2(m, S)$  over EGOE(1+2)-s ensemble assuming that  $h(1)$  is fixed and the final result is as follows. First the ensemble averaged variance is

$$\overline{\sigma_H^2(m, S)} = \overline{\sigma_{h(1)}^2(m, S)} + \overline{\sigma_{V(2)}^2(m, S)}. \quad (6)$$

The propagation formula for  $\sigma_{h(1)}^2$  is simple,

$$\sigma_{h(1)}^2(m, S) = \frac{(\Omega + 2)m(\Omega - m/2) - 2\Omega S(S + 1)}{(\Omega - 1)(\Omega + 1)} \sigma_{h(1)}^2\left(1, \frac{1}{2}\right). \quad (7)$$

The two parts  $V^{s=0}(2)$  and  $V^{s=1}(2)$  of  $V(2)$  will have a scalar part, an effective one-body part and an irreducible two-body part denoted by  $V^{s,\nu}(2)$ , with  $\nu=0, 1$ , and  $2$ , respectively, with respect to  $U(N) \supset U(\Omega) \otimes SU(2)$  algebra. The two  $\nu=0$  parts generate the centroids and they can be identified from Eq. (4). As the  $\nu$  decomposition is an orthogonal decomposition, we have

$$\overline{\sigma_{V(2)}^2(m, S)} = \sum_{s=0,1} \lambda_s^2 \sum_{\nu=1,2} \overline{\langle [V^{s,\nu}(2)]^2 \rangle^{m,S}}. \quad (8)$$

As seen from Eq. (8) of [26], for evaluating  $\overline{\langle [V^{s,\nu=1}(2)]^2 \rangle^{m,S}}$  we need  $\sum_{i,j} \lambda_{i,j}^2(s)$  where the  $\lambda(s)$ 's are the so-called induced one-particle matrix elements generated by  $V^s$ ,

$$\begin{aligned} \lambda_{i,i}(s) &= \sum_j V_{ijij}^s (1 + \delta_{ij}) - (\Omega)^{-1} \sum_{k,l} V_{klkl}^s (1 + \delta_{kl}), \\ \lambda_{i,j}(s) &= \sum_k \sqrt{(1 + \delta_{ki})(1 + \delta_{kj})} V_{kikj}^s \quad \text{for } i \neq j. \end{aligned} \quad (9)$$

Similarly for evaluating  $\overline{\langle [V^{s,\nu=2}(2)]^2 \rangle^{m,S}}$ , we need  $\overline{\langle [V^{s,\nu=2}(2)]^2 \rangle^{2,S}}$ . First, applying the fact that the  $V^s$  matrix elements are independent Gaussian random variables with zero center and variance unity (except for the diagonal matrix elements it is 2) and simplifying using Eq. (9), we obtain

$$\begin{aligned} \sum_{i,j} \overline{\lambda_{i,j}^2(0)} &= (\Omega - 1)(\Omega + 2)^2, \\ \sum_{i,j} \overline{\lambda_{i,j}^2(1)} &= (\Omega - 1)(\Omega - 2)(\Omega + 2). \end{aligned} \quad (10)$$

Also,  $\overline{\langle [V^s(2)]^2 \rangle^{2,S}} = [d(2, s) + 1]$ . This along with Eq. (8) of [26] and Eqs. (4) and (10) will give  $\overline{\langle [V^{s,\nu=2}(2)]^2 \rangle^{2,S}}$ ,

$$\begin{aligned} \overline{\langle [V^{s=0,\nu=2}(2)]^2 \rangle^{2,0}} &= \frac{1}{2}(\Omega - 1)(\Omega + 2), \\ \overline{\langle [V^{s=1,\nu=2}(2)]^2 \rangle^{2,1}} &= \frac{(\Omega - 3)(\Omega^2 + \Omega + 2)}{2(\Omega - 1)}. \end{aligned} \quad (11)$$

Substituting the results in Eqs. (4), (8), (10), and (11) in Eq. (8) of [26] gives the final result,

$$\begin{aligned} \overline{\sigma_{V(2)}^2(m, S)} &= \frac{\lambda_0^2}{\Omega(\Omega + 1)/2} \left[ \frac{\Omega + 2}{\Omega + 1} Q^1(\{2\}; m, S) \right. \\ &\quad \left. + \frac{\Omega^2 + 3\Omega + 2}{\Omega^2 + 3\Omega} Q^2(\{2\}; m, S) \right] \\ &\quad + \frac{\lambda_1^2}{\Omega(\Omega - 1)/2} \left[ \frac{\Omega + 2}{\Omega + 1} Q^1(\{1^2\}; m, S) \right. \\ &\quad \left. + \frac{\Omega^2 + \Omega + 2}{\Omega^2 + \Omega} Q^2(\{1^2\}; m, S) \right]; \end{aligned}$$

$$Q^1(\{2\}; m, S) = [(\Omega + 1)P^0(m, S)/16][m^x(m + 2)/2 + \langle S^2 \rangle],$$

$$Q^2(\{2\}; m, S) = [\Omega(\Omega + 3)P^0(m, S)/32][m^x(m^x + 1) - \langle S^2 \rangle],$$

$$\begin{aligned} Q^1(\{1^2\}; m, S) &= \frac{(\Omega - 1)}{16(\Omega - 2)} [(\Omega + 2)P^1(m, S)P^2(m, S) \\ &\quad + 8\Omega(m - 1)(\Omega - 2m + 4)\langle S^2 \rangle], \end{aligned}$$

$$\begin{aligned} Q^2(\{1^2\}; m, S) &= \frac{\Omega}{8(\Omega - 2)} [(3\Omega^2 - 7\Omega + 6)(\langle S^2 \rangle)^2 \\ &\quad + 3m(m - 2)m^x(m^x - 1)(\Omega + 1)(\Omega + 2)/4 \\ &\quad + \langle S^2 \rangle \{-mm^x(5\Omega - 3)(\Omega + 2) \\ &\quad + \Omega(\Omega - 1)(\Omega + 1)(\Omega + 6)\}], \end{aligned}$$

$$P^2(m, S) = 3m^x(m - 2)/2 - \langle S^2 \rangle, \quad m^x = \left( \Omega - \frac{m}{2} \right). \quad (12)$$

Note that the  $\nu=1$  terms (they correspond to the  $Q^1$ 's) are  $1/\Omega^2$  times smaller as compared to the  $\nu=2$  terms (they correspond to the  $Q^2$ 's). Therefore in the dilute limit defined by  $\Omega \rightarrow \infty$ ,  $m \rightarrow \infty$ ,  $m/\Omega \rightarrow 0$  and  $m \gg S$ , the  $V^{s=0,1:\nu=2}$  parts determine the variances  $\sigma_H^2(m, S)$ . As a result, formula for the ensemble averaged variances given in [25] is same as the sum of the two  $\nu=2$  terms in Eq. (12).

In most of the numerical examples discussed in the remaining part of the paper (except in Appendix B) we employ  $\lambda_0 = \lambda_1 = \lambda$  and for this  $\overline{\sigma_{V(2)}^2(m, S)}$  takes the form

$$\overline{\sigma_{V(2)}^2(m, S)} \xrightarrow{\lambda_0 = \lambda_1 = \lambda} \lambda^2 P(\Omega, m, S);$$

$$\begin{aligned} P(\Omega, m, S) &= \frac{1}{\Omega(\Omega + 1)/2} \left[ \frac{\Omega + 2}{\Omega + 1} Q^1(\{2\}; m, S) \right. \\ &\quad \left. + \frac{\Omega^2 + 3\Omega + 2}{\Omega^2 + 3\Omega} Q^2(\{2\}; m, S) \right] \\ &\quad + \frac{1}{\Omega(\Omega - 1)/2} \left[ \frac{\Omega + 2}{\Omega + 1} Q^1(\{1^2\}; m, S) \right. \\ &\quad \left. + \frac{\Omega^2 + \Omega + 2}{\Omega^2 + \Omega} Q^2(\{1^2\}; m, S) \right]. \end{aligned} \quad (13)$$

Note that we are showing  $\Omega$  explicitly in the formula for the variance propagator  $P(\Omega, m, S)$  as  $\Omega$  plays an important role in determining the transition markers. Figure 2 shows a plot

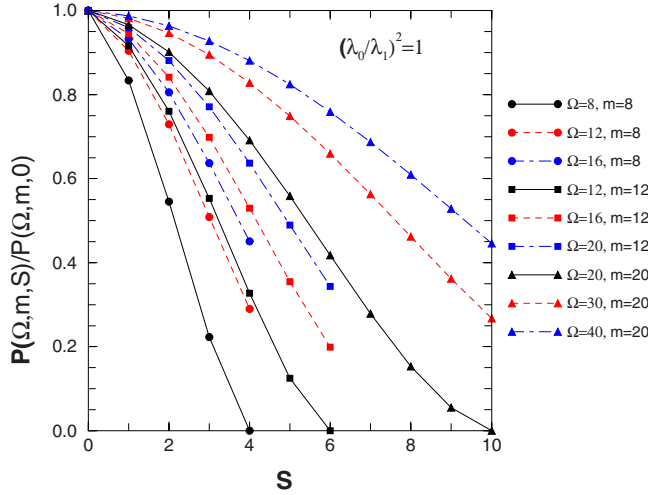


FIG. 2. (Color online) Variance propagator  $P(\Omega, m, S)$  vs  $S$  for different values of  $\Omega$  and  $m$ . Equation (13) gives the formula for  $P(\Omega, m, S)$ .

of  $P(\Omega, m, S)/P(\Omega, m, 0)$  vs  $S$  for various values of  $m$  and  $\Omega$ . As seen from Fig. 2,  $P(\Omega, m, S)$  decreases with spin and this plays an important role in understanding the properties of EGOE(1+2)-s as will be seen in the following Sections. As an aside let us point out that Eqs. (5) and (12) give for EGOE(2)-s, the exact formula for the normalized cross correlations  $\Sigma_{11}$  in the energy centroids with different  $(m, S)$  values where

$$\Sigma_{11}(m, S; m', S') = \frac{\overline{\langle H(2) \rangle^{m, S} \langle H(2) \rangle^{m', S'}}}{[\overline{\langle H^2(2) \rangle^{m, S} \langle H^2(2) \rangle^{m', S'}}]^{1/2}}; \quad (14)$$

$$H(2) = V(2).$$

It is important to mention here that the mathematical treatment of the embedded Gaussian unitary ensemble of two-body interactions with spin degree of freedom [EGUE(2)-s] is comparatively easier than for EGOE(2)-s. For the EGUE(2)-s ensemble, using  $U(N) \supset U(\Omega) \otimes SU(2)$  Wigner-Racah algebra, exact analytical formulas are derived for the ensemble averaged spectral variances, cross correlations in energy centroids as defined by Eq. (14) and also for the cross correlations in spectral variances as given by

$$\Sigma_{22}(m, S; m', S') = \frac{\overline{\langle [H(2)]^2 \rangle^{m, S} \langle [H(2)]^2 \rangle^{m', S'}}}{\overline{\langle [H(2)]^2 \rangle^{m, S}} \times \overline{\langle [H(2)]^2 \rangle^{m', S'}}} - 1$$

[50]. In addition, the ensemble averaged excess parameter for the fixed- $(m, S)$  density of states is given in terms of  $SU(\Omega)$  Racah coefficients but general analytical formulas for these Racah coefficients are not yet available [50]. For the ensemble averaged variances, comparing Eq. (12) with Eq. (19) of [50], it is seen that the leading-order terms are the same for both EGOE(2)-s and EGUE(2)-s. The first-order correction for EGOE(2)-s is  $1/\Omega^2$  times smaller compared to the leading term. Similarly, comparing the formulas for  $\Sigma_{11}$  it is seen that to the leading order the EGOE(2)-s result is

twice that of EGUE(2)-s. Both these results are identical to the results derived for EGOE(2) and EGUE(2) for spinless fermion systems [6]. Therefore drawing on the results in [6], we conjecture that  $\Sigma_{22}$  for EGOE(2)-s will also be twice that of EGUE(2)-s to the leading order.

#### IV. POISSON (OR CLOSE TO POISSON) TO GOE TRANSITION IN LEVEL FLUCTUATIONS

Fluctuations in the eigenvalues of a fixed- $(m, S)$  spectrum derive from the two and higher point correlation functions. For example, the two-point function is

$$S^{\rho: m, S}(E_i, E_f) = \overline{\rho^{m, S}(E_i) \rho^{m, S}(E_f)} - \overline{\rho^{m, S}(E_i)} \overline{\rho^{m, S}(E_f)}. \quad (15)$$

The commonly used Dyson-Mehta  $\Delta_3$  statistic is an exact two-point measure while variance  $\sigma^2(0)$  of the nearest-neighbor spacing distribution (NNSD) is essentially a two-point measure [4]. Note that, due to an unfortunate convention as stated in the footnote 14 of [4], the variance of the NNSD is  $\sigma^2(0)$ , the second nearest  $\sigma^2(1)$  etc. In all the discussion in this Sec. and all other remaining Secs. V–VIII (except Appendix B), we use  $\lambda_0 = \lambda_1 = \lambda$ , i.e., we employ EGOE(1+2)-s Hamiltonian,

$$H_\lambda = h(1) + \lambda[V^{s=0}(2) + V^{s=1}(2)]. \quad (16)$$

The NNSD and  $\Delta_3$  statistics show Poisson character in general [51] for very small values of  $\lambda$  due to the presence of many good quantum numbers defined by  $h(1)$ . As the value of  $\lambda$  increases, there is delocalization in the Fock space, i.e., the eigenstates spread over all the basis states leading to complete mixing of the basis states. Hence, one expects GOE behavior for large  $\lambda$  values.

For a 20 member EGOE(1+2)-s ensemble with  $\Omega = m = 8$  and spins  $S = 0, 1$ , and  $2$ , we have constructed NNSD and  $\Delta_3$  for various  $\lambda$  values changing from 0.01 to 0.3. In the calculations: (i) the spectrum for each member of the ensemble is unfolded using ED corrected Gaussian for the eigenvalue density so that the average spacing is unity; (ii) we drop 5% of the levels from the two spectrum ends; (iii) with this we have constructed the ensemble averaged NNSD histograms and calculated their variances  $\sigma^2(0)$ ; (iv) for the  $\Delta_3$  statistic, overlap interval of 0.5 (for the unfolded spectrum) is used and  $\overline{\Delta_3(L)}$  for  $L \leq 60$  are calculated following Ref. [52];  $L$  is the energy interval, measured in units of average level spacing, over which  $\Delta_3$  is calculated. Results for NNSD and  $\Delta_3$  statistic are shown in Figs. 3 and 4, respectively. As mentioned in Sec. III A, in our calculation the mean-field Hamiltonian is of a special form defined by the sp energies  $\epsilon_i = i + 1/i$ . For this Hamiltonian, it is easy to see that in the dilute regime, the majority of many-body eigenvalues approach a perturbed picket-fence spectrum. Away from the dilute limit, the spectrum is not picket-fence and deviates from Poisson as can be seen from Figs. 3 and 4. However, if we had used sp energies drawn from the center of a GOE or from the eigenvalues of an irregular system, the fluctuations will be generically Poisson [51]. Therefore we call the transition seen in Figs. 3 and 4, Poisson to GOE transition and it

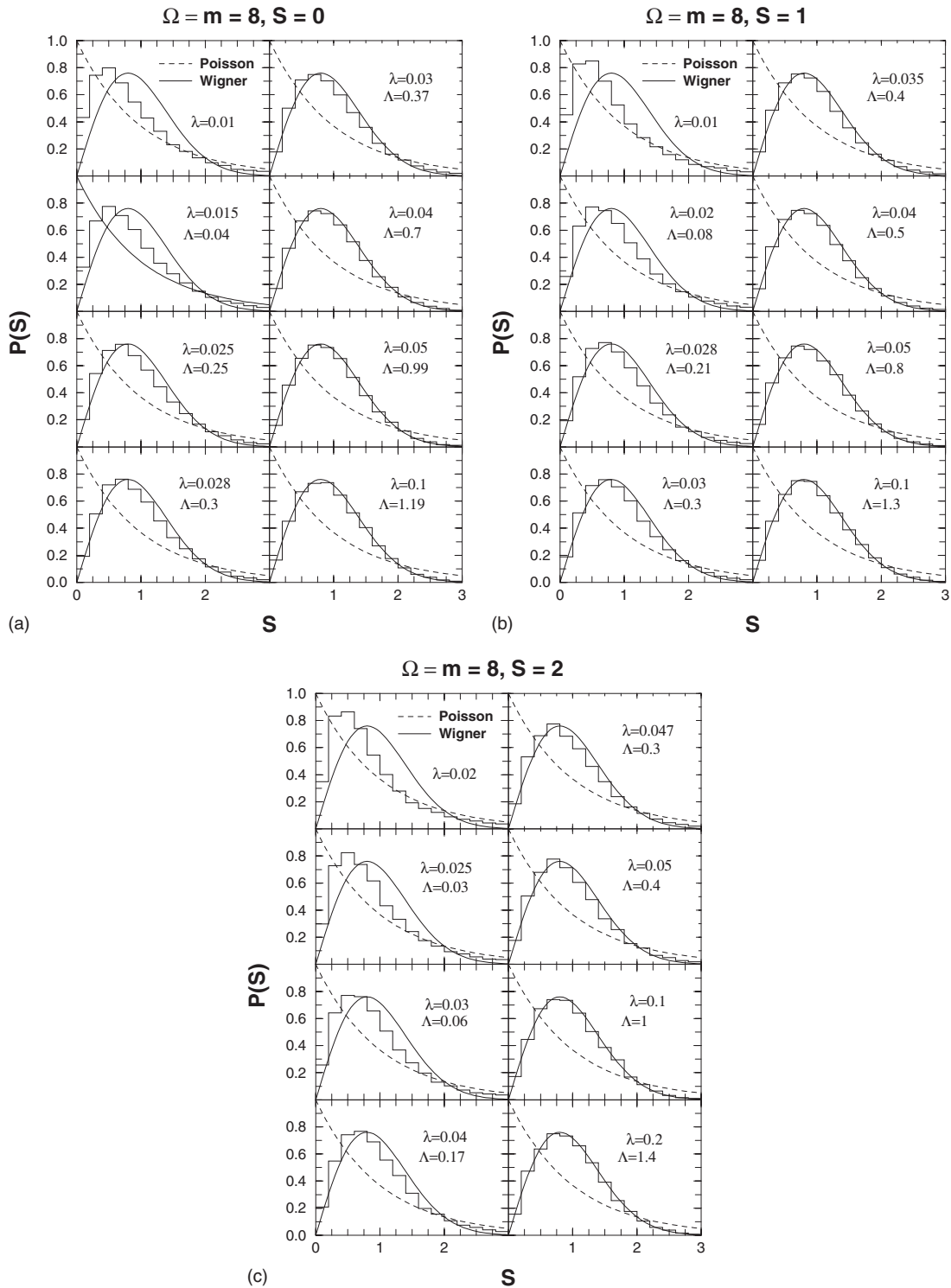


FIG. 3. NNSD for a 20 member EGOE(1+2)-s ensemble with  $\Omega = m = 8$  and spins  $S = 0, 1$  and  $2$ , respectively. Calculated NNSD are compared to the Poisson and Wigner (GOE) forms. Values of the interaction strength  $\lambda$  and the transition parameter  $\Lambda$  are given in the figure. The chaos marker  $\lambda_c$  corresponds to  $\Lambda = 0.3$ . Bin size for the histograms is  $0.2$ . As discussed in the text, for very small values of  $\lambda$ , the NNSD, for the sp spectrum employed in the calculations, is not strictly a Poisson. Therefore, the  $\Lambda$  values are not given for  $\lambda = 0.01$  for spins  $S = 0$  and  $1$  and for  $\lambda = 0.02$  for spin  $S = 2$ .

should be kept in mind that, the sp spectrum we have chosen gives level fluctuations that are close to Poisson but not strictly Poisson for  $\lambda = 0$ . For further discussion we focus on the NNSD and its variance  $\sigma^2(0)$ .

As we increase  $\lambda$ , NNSD changes rapidly from a form close to Poisson to a form close to that of GOE (Wigner distribution) as seen from Fig. 3. However, the complete convergence to GOE form is very slow. Therefore, although

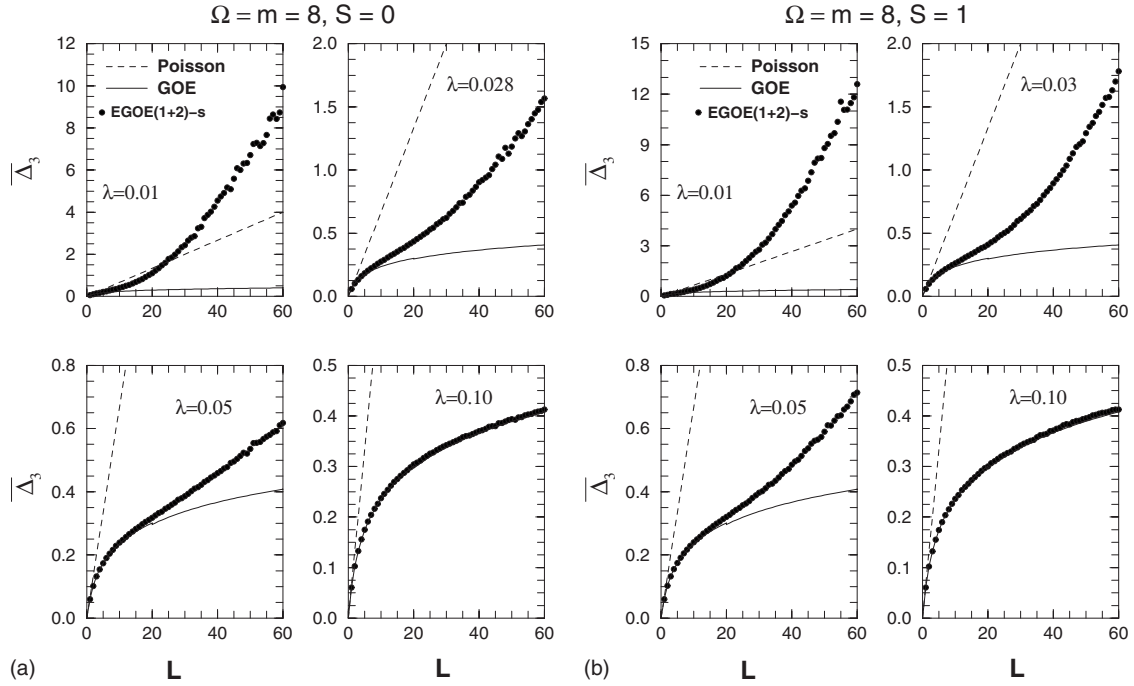


FIG. 4.  $\overline{\Delta}_3(L)$  vs  $L$  for a 20 member EGOE(1+2)-s ensemble with  $\Omega=m=8$  and spins  $S=0$  and 1. Calculated results are compared with the Poisson and GOE forms.

the transition to GOE in level fluctuations is not a phase transition, we can still define a transition point  $\lambda=\lambda_c$  where Poisson-like fluctuations start changing to GOE character and we need a criterion to determine  $\lambda_c$ . For this purpose we employ  $\sigma^2(0)$  given by a simple  $2 \times 2$  random matrix model for Poisson to GOE transition [53] as used in some of the earlier studies [46]. In this model, in terms of a transition parameter  $\Lambda$  ( $\Lambda$  is mean squared admixing GOE matrix element divided by the square of the mean spacing  $D_0$  of the Poisson spectrum),  $\sigma_{P \rightarrow GOE}^2(0:\Lambda) = (8\Lambda + 2) / [\pi(\Psi(-0.5, 0, 2\Lambda))]^2 - 1$ . Here  $\Psi$  is the Kummer function. It can be argued that the transition to GOE is nearly complete for  $\Lambda \sim 0.3$  which corresponds to NNSD variance  $\sigma^2(0) = 0.37$ . A plot of  $\sigma_{P \rightarrow GOE}^2(0:\Lambda)$  vs  $\Lambda$  [53] shows that the variance decreases fast from Poisson value  $\sigma^2(0) = 1$  up to  $\Lambda \sim 0.37$  and then converges slowly to the GOE value  $\sigma^2(0) = 0.27$ . For the NNSD that are constructed for various EGOE(1+2)-s examples, the calculated  $\sigma^2(0)$  are used to deduce, from the  $2 \times 2$  matrix formula, the values of  $\Lambda$ . In Fig. 3, the values of the  $\Lambda$  parameter are given for different  $\lambda$  values and it is seen that the transition point  $\lambda_c$  is 0.028, 0.030, and 0.047 for  $S=0, 1$ , and 2, respectively. In Fig. 4, we show  $\overline{\Delta}_3(L)$  vs  $L$  for some values of  $\lambda$  and clearly there is a transition to GOE statistics. It should be stressed that one expects the  $\lambda_c$  needed to approach GOE statistics for  $\overline{\Delta}_3(L)$  to scale as  $L^{1/2}$  [54] although the scaling of  $\lambda_c$  with other parameters  $(m, S, \Omega)$  will be same for any given  $L$ . In the present example, up to  $L=20$ , the  $\lambda_c$  deduced from NNSD could be considered as the transition point for  $\overline{\Delta}_3(L)$ . However the  $L$  dependence of  $\lambda_c$  is not probed further in the present paper.

For a qualitative understanding of the variation of  $\lambda_c$  with spin  $S$ , it is plausible to use the same arguments used for spinless fermion systems and they are based on perturbation theory [15]. As  $\lambda$  is increased from zero, the  $m$  particle states

generated by  $h(1)$  will be mixed by  $V(2)$  and in lowest-order perturbation the first stage of mixing will be between states that are directly coupled by the two-body interaction. Poisson to GOE transition occurs when  $\lambda$  is of the order of the spacing  $\Delta_c$  between the  $m$  particle states that are directly coupled by the two-body interaction. Given the two-particle spectrum span to be  $B_2$  and the number of fixed- $(m, S)$  states directly coupled by the two-body interaction to be  $K(\Omega, m, S)$ , we have  $\Delta_c(\Omega, m, S) \propto B_2 / K(\Omega, m, S)$  and therefore,  $\lambda_c \propto B_2 / K(\Omega, m, S)$ . Using the  $h(1)$  spectrum, it is easy to see that  $B_2 \propto \Omega$ . Following the arguments in [30] (see also [25]), the spectral variances generated by  $V(2)$  can be written as  $\sigma_{V(2)}^2(m, S) \approx \lambda^2 K(\Omega, m, S)$  and applying Eq. (13) gives  $K(\Omega, m, S) \approx P(\Omega, m, S)$ . With this, we have

$$\lambda_c(S) \propto \frac{\Omega}{P(\Omega, m, S)}. \quad (17)$$

From the results in Fig. 2, it is clear that  $\lambda_c$  should increase with spin  $S$ . For  $\Omega=m=8$ , Eq. (17) and the formula for  $P(\Omega, m, S)$  gives  $P(8, 8, S=1) / P(8, 8, S=0) = 0.834$  and  $P(8, 8, S=2) / P(8, 8, S=0) = 0.55$ . These and the result  $\lambda_c(S=0) = 0.028$  from Fig. 3 will give  $\lambda_c(S=1) = 0.034$  and  $\lambda_c(S=2) = 0.05$ . These predictions are close to the numerical results shown in Fig. 3. Therefore Eq. (17) gives a good qualitative understanding of the  $\lambda_c(S)$  variation with  $S$ . In the dilute limit (sometimes also called asymptotic limit), as defined just after Eq. (12), it is easily seen that  $P(\Omega, m, S) \rightarrow m^2 \Omega^2$  and hence  $\lambda_c \rightarrow 1 / m^2 \Omega$ . Thus we recover the result known [15] for spinless fermion systems as a limiting case.

### V. BREIT-WIGNER TO GAUSSIAN TRANSITION IN STRENGTH FUNCTIONS

Wavefunction structure is understood usually in terms of strength functions  $[F_k(E)]$  and information entropy

## EGOE(1+2)-s

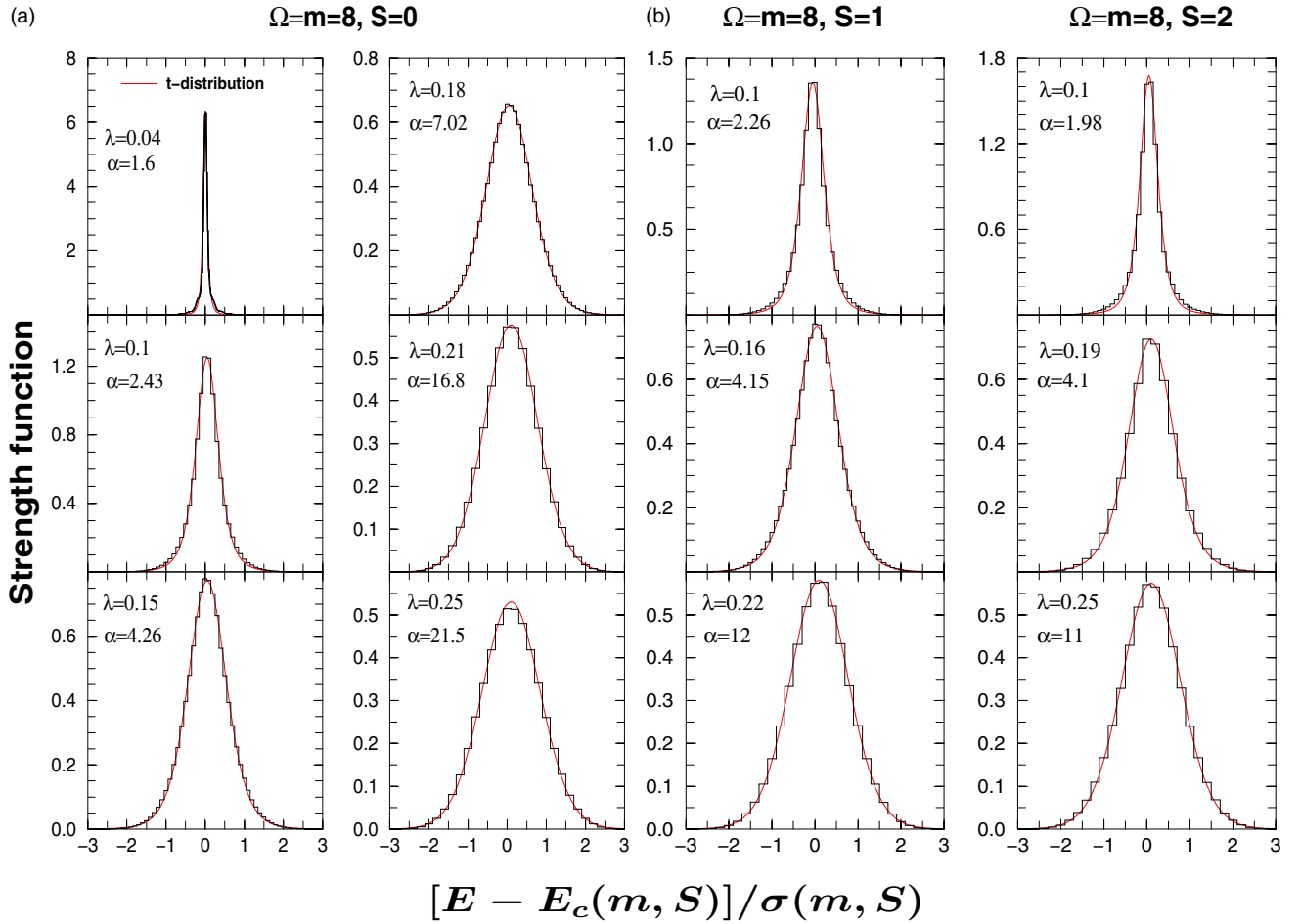


FIG. 5. (Color online) Strength functions as a function of  $\lambda$  for a 20 member EGOE(1+2)-s ensemble. Calculations (histograms) are for a  $\Omega=m=8$  system with spins  $S=0, 1$  and  $2$ . Note that the widths  $\sigma_{F_k}(m, S)$  of the strength functions are different from the spectral widths  $\sigma(m, S)$ . Continuous curves in the figures correspond to the  $t$ -distribution given by Eq. (21). See text for details.

$[S^{info}(E)]$ . Both of these are basis dependent. In our (also by all others [26–28,30,31]) construction of the  $H$  matrices, the basis states chosen are eigenstates of both  $\hat{h}(1)$  and  $\hat{S}^2$  operators (we drop  $M_S^{min}$  everywhere although all the states have  $M_S=M_S^{min}$ ). Given the mean-field  $h(1)$  basis states (denoted by  $|k\rangle$ ) expanded in the  $H$  eigenvalue ( $E$ ) basis,

$$|k, S, M_S\rangle = \sum_E C_{k,S}^{E,S} |E, S, M_S\rangle, \quad (18)$$

the strength functions  $F_{k,S}(E, S)$  and information entropy  $S^{info}(E, S)$  are defined by

$$F_{k,S}(E, S) = \sum_{E'} |C_{k,S}^{E',S}|^2 \delta(E - E') = |C_{k,S}^{E,S}|^2 d(m, S) \rho^{m,S}(E),$$

$$S^{info}(E, S) = - \frac{1}{d(m, S) \rho^{m,S}(E)} \times \sum_{E'} \sum_k |C_{k,S}^{E',S}|^2 \ln |C_{k,S}^{E',S}|^2 \delta(E - E'), \quad (19)$$

where  $|C_{k,S}^{E,S}|^2$  denotes the average of  $|C_{k,S}^{E,S}|^2$  over the eigen-

states with the same energy  $E$ . The strength functions give the spreading of the basis states over the eigenstates. For  $\lambda=0$ , the strength functions will be  $\delta$ -functions at the  $h(1)$  eigenvalues. As  $\lambda$  increases from zero, the strength functions first change from  $\delta$ -function form to BW form at  $\lambda=\lambda_\delta$  where  $\lambda_\delta$  is very small; see Eq. (22) ahead. The BW form, with  $\Gamma$  denoting the spreading width, is defined by

$$F_{k,BW}(E) = \frac{1}{2\pi} \frac{\Gamma}{(E - \xi_k)^2 + \Gamma^2/4}. \quad (20)$$

The energies  $\xi_k = \langle \phi_k | H | \phi_k \rangle$  are the diagonal matrix elements of  $H$  and they are the basis-state energies. Information entropy  $S^{info}$  is a measure of complexity or chaos in wavefunctions and the GOE value for  $\exp[S^{info}(E, S)]$  is  $0.48d(m, S)$  independent of  $E$ . Our purpose is to investigate the change in  $F_{k,S}(E, S)$  and  $S^{info}(E, S)$  as we change  $\lambda$ . In the present section we consider strength functions and in the next Sec. information entropy.

Figure 5 shows strength functions as a function of  $\lambda$  for 8 particles in 8 sp levels ( $\Omega=m=8$ ) with spins  $S=0, 1$ , and  $2$ . The centroids ( $\epsilon$ ) of the  $\xi_k$  spectra are same as that of the

eigenvalue ( $E$ ) spectra but their widths are different. In the calculations,  $E$  and  $\xi_k$  are zero centered for each member and scaled by the width of the eigenvalue spectrum. The new energies are called  $\hat{E}$  and  $\hat{E}_k$ , respectively. For each member  $|C_{k,S}^{E,S}|^2$  are summed over the basis states in the energy window  $\hat{E}_k \pm \Delta_k$  and then the ensemble averaged  $F_k(\hat{E}, S)$  vs  $\hat{E}$  are constructed as histograms. We have chosen  $\Delta_k=0.025$  for  $\lambda < 0.1$  and beyond this  $\Delta_k=0.1$ . In the plots  $\int F_k(\hat{E}, S) d\hat{E} = 1$ . Clearly, strength functions exhibit transition from BW to Gaussian form. To describe this transition, a simple linear interpolation of BW and Gaussian forms, with three parameters, as employed in [55] could be used. However, an alternative form is given by the one-parameter  $t$ -distribution well known in statistics and it is used in [22]. In the following we employ the  $t$ -distribution.

Student's  $t$ -distribution, with a shape parameter  $\alpha$ , such that  $\alpha=1$  gives BW and  $\alpha \rightarrow \infty$  gives Gaussian, is a good interpolating function for BW to Gaussian transition and it is given by

$$F_k^{stud}(E, S) dE = \frac{(\alpha\beta)^{\alpha-1/2} \Gamma(\alpha)}{\sqrt{\pi} \Gamma(\alpha-1/2) [(E-E_k)^2 + \alpha\beta]^\alpha} dE. \quad (21)$$

The parameter  $\beta$  defines the energy spread and hence, it is determined by the variance of the strength function  $\sigma_{F_k}^2$ , i.e.,  $\beta = \sigma_{F_k}^2 (2\alpha-3)/\alpha$  for  $\alpha > 1.5$ . For  $\alpha \leq 1.5$ , the spreading width determines the parameter  $\beta$ . Numerical results for the strength functions are compared with the best fit  $F_k^{stud}(E, S)$  and they are shown as continuous curves in Fig. 5 along with the values of the parameter  $\alpha$ . Although only the results for  $S=0, 1, 2$  and  $\hat{E}_k=0$  are shown in the figures, we have also performed calculations for  $S=0$  with  $\hat{E}_k = \pm 0.5$ . As seen from the figures, the fits are excellent over a wide range of  $\lambda$  values. The parameter  $\alpha$  rises slowly up to  $\lambda_F$ , then it increases sharply (for  $\alpha > 16$  the curves are indistinguishable from Gaussian). Following [22], the criterion  $\alpha \sim 4$  defines the transition point  $\lambda_F$ . From the results in Fig. 5 it is seen that the transition point  $\lambda_F$  is 0.15 and 0.16 for  $S=0$  and 1, respectively. In addition,  $\lambda_F=0.19$  for  $S=2$  (for  $\lambda=0.075$  and 0.15,  $\alpha=1.69$  and 2.73, respectively). Similarly for  $S=0$  and  $\hat{E}_k = \pm 0.5$ , the  $\lambda_F$  value is 0.16. Thus  $\lambda_F$  increases slowly with  $\hat{E}_k$ .

For a qualitative understanding of the variation of  $\lambda_F$  with spin  $S$ , we consider the spreading width  $\Gamma(S)$  and the inverse participation ratio (IPR)  $\zeta(S)$ . First, Fermi golden rule gives  $\Gamma(S) = 2\pi\lambda^2/D(S)$  with  $D(S) = \Delta_c(\Omega, m, S)$  as established in [16]. Therefore, using Eq. (17) gives  $\Gamma(S) \propto 2\pi\lambda^2 P(\Omega, m, S)/\Omega$ . Similarly,  $\zeta(S) \sim \Gamma(S)/\Delta_m(S)$  with  $\Delta_m(S)$  being the average spacing of the  $m$  particle fixed- $S$  spectrum. The total spectrum span considering only  $h(1)$  is  $B_m \propto m\Omega$  and therefore  $\Delta_m(S) \propto m\Omega/d(m, S)$ . In the BW domain,  $\Gamma(S)$  and  $\zeta(S)$  should be such that (i)  $\Gamma(S) < f_0 B_m$  and (ii)  $\zeta(S) \gg 1$  where  $f_0 < 1$ . Condition (i) gives,  $\lambda^2 < C_0 m \Omega^2 / P(\Omega, m, S)$  and condition (ii) gives,  $\lambda^2 \gg B_0 m \Omega^2 / P(\Omega, m, S) d(m, S)$ . Note that the constants  $C_0$  and  $B_0$  are positive. Therefore,

$$\begin{aligned} \sqrt{\frac{B_0 m \Omega^2}{P(\Omega, m, S) d(m, S)}} \ll \lambda < \sqrt{\frac{C_0 m \Omega^2}{P(\Omega, m, S)}} \\ \Rightarrow \lambda_F(S) \propto \sqrt{\frac{m \Omega^2}{P(\Omega, m, S)}}. \end{aligned} \quad (22)$$

This equation shows that just as  $\lambda_c$ , the marker  $\lambda_F$  is essentially determined by the variance propagator  $P(\Omega, m, S)$ . Also as  $\lambda$  increases from zero, the BW form sets in fast as  $d(m, S)$  is usually very large. From the results in Fig. 2, it is clear that  $\lambda_F$  should increase with  $S$ . This prediction is close to the numerical results shown in Fig. 5. Equation (22) with the result  $\lambda_F(S=0)=0.15$  gives  $\lambda_F(S=1)=0.16$  and  $\lambda_F(S=2)=0.2$ . Therefore Eq. (22) gives a good qualitative understanding of  $\lambda_F(S)$  variation with  $S$  just as for  $\lambda_c(S)$ . In the dilute limit with  $P(\Omega, m, S) \rightarrow m^2 \Omega^2$ , we have  $\lambda_F \rightarrow 1/\sqrt{m}$  and thus reducing to the result known [18] for spinless fermion systems.

## VI. INFORMATION ENTROPY AND DUALITY MARKER

Figure 6 shows information entropy  $S^{info}(E, S)$  as a function of  $E$  for a 20 member EGOE(1+2)-s ensemble with spins  $S=0$  and 1 and for different  $\lambda$  values. These results are compared with the EGOE(1+2) formula for  $S^{info}$  given in [17] (strictly valid only for  $\lambda > \lambda_F$ ) by replacing the fixed- $m$  variances by fixed- $(m, S)$  variances,

$$\begin{aligned} \exp(S^{info}(E, S) - S_{GOE}^{info}) \xrightarrow{\text{EGOE}(1+2)\text{-s}} \sqrt{1 - \xi^2} \exp\left(\frac{\xi^2}{2}\right) \\ \times \exp\left(-\frac{\xi^2 \hat{E}^2}{2}\right) \end{aligned} \quad (23a)$$

$$\xi^2 = 1 - \frac{\sigma_{\text{off-diagonal}}^2(m, S)}{\sigma^2(m, S)} \sim \frac{\sigma_{h(1)}^2(m, S)}{\sigma_{h(1)}^2(m, S) + \sigma_{V(2)}^2(m, S)}. \quad (23b)$$

Note that  $\hat{E}$  is defined just before Eq. (3) and  $\xi$  is a correlation coefficient. The results given by Eq. (23a) are compared with the numerical results in Fig. 6. It is seen that the numerical results for  $\lambda \geq \lambda_F$  are described well by the EGOE formula. There are deviations at the tails because the result given by Eq. (23a) assumes Gaussian form for the strength functions while in practice there will be corrections to the Gaussian form. Thus results of EGOE(1+2) extend to EGOE(1+2)-s with parameters calculated in  $(m, S)$  spaces. Similar analysis was done for number of principal components or IPR in [26].

For the EGOE(1+2)-s Hamiltonian, two asymptotic natural basis emerge and they are (i) the noninteracting basis defined by  $\lambda_0 = \lambda_1 = 0$  and (ii) the infinite interaction strength basis defined by  $\lambda_0 = \lambda_1 = \infty$ . In principle two more basis defined by  $\lambda_0 = 0, \lambda_1 = \infty$  and  $\lambda_0 = \infty, \lambda_1 = 0$  are possible but they are not considered in the present Section. Therefore just as in the previous discussion we put  $\lambda_0 = \lambda_1 = \lambda$ . An important question is: is there a point  $\lambda = \lambda_d \geq \lambda_F$  where quantities de-

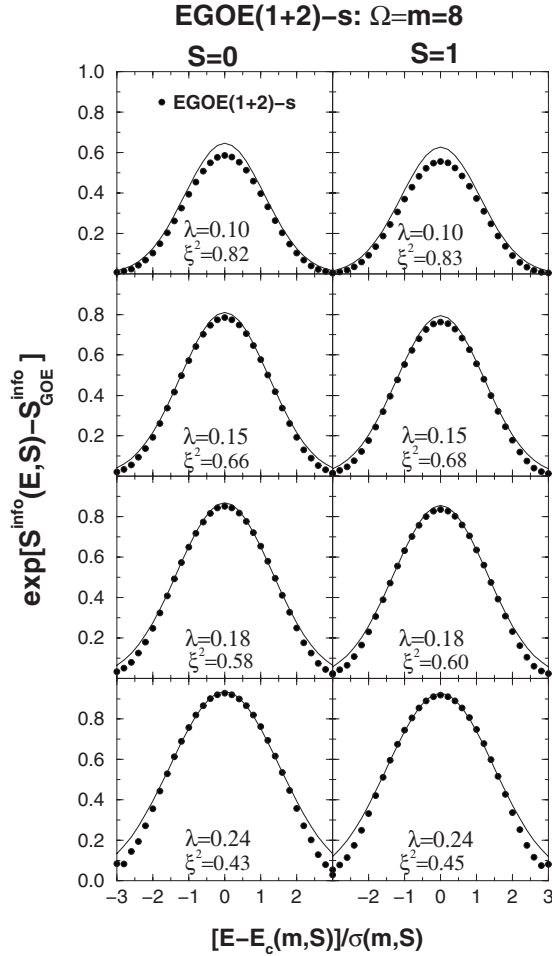


FIG. 6.  $\exp[S^{\text{info}}(E,S) - S_{\text{GOE}}^{\text{info}}]$  for a 20 member EGOE(1+2)-s ensemble with  $\Omega=m=8$  and spins  $S=0$  and  $1$  for different  $\lambda$  values. Values averaged over bin size  $0.2$  are shown as filled circles. The continuous curves correspond to Eq. (23a). See text for details.

fining wavefunction properties like entropy, strength functions, temperature etc. are basis independent [18,22]. To examine this question, we compare  $S^{\text{info}}(E,S)$  in  $\lambda=0$  and  $\lambda=\infty$  basis by varying  $\lambda$ . In the  $\lambda=0$  basis,  $S^{\text{info}}(E,S)$  is determined by Eq. (23a) with the correlation coefficient  $\xi^2 = \xi_0^2$  defined in Eq. (23b). Similarly, in the  $\lambda=\infty$  basis, Eq. (23a) applies with  $\xi^2 = \xi_\infty^2 = \sigma_{V(2)}^2(m,S) / [\sigma_{h(1)}^2(m,S) + \sigma_{V(2)}^2(m,S)]$ ; note that  $\sigma_{V(2)}^2(m,S)$  depends on  $\lambda^2$ . Therefore we can determine  $\lambda_d$  by using the condition that  $\xi_0^2 = \xi_\infty^2$  (this is equivalent to the condition that the spreadings produced by  $h(1)$  and  $V(2)$  are equal). Then we have  $\xi^2 = \xi_0^2 = \xi_\infty^2 = 0.5$  at  $\lambda = \lambda_d$ ; see [22] for more details. Further, it can be argued that the duality region (defined by  $\lambda \sim \lambda_d$ ) corresponds to the thermodynamic region for finite quantum systems and this will be discussed in Sec. VII.

Figure 7 shows numerical results for the information entropy in the  $h(1)$  and  $V(2)$  basis for a 20 member EGOE(1+2)-s ensemble with  $\Omega=m=8$  and spins  $S=0$  and  $1$  for different  $\lambda$  values ranging from  $\lambda=0.18$  to  $0.3$ . It is seen from Fig. 7 that the duality marker  $\lambda_d=0.21$  for spin  $S=0$  and  $0.22$  for  $S=1$ . For  $\lambda$  values below and above  $\lambda_d$  clearly there are differences in  $S^{\text{info}}(E,S)$  in the two basis. The  $S^{\text{info}}(E,S)$  values in the  $h(1)$  basis are smaller compared to those in the

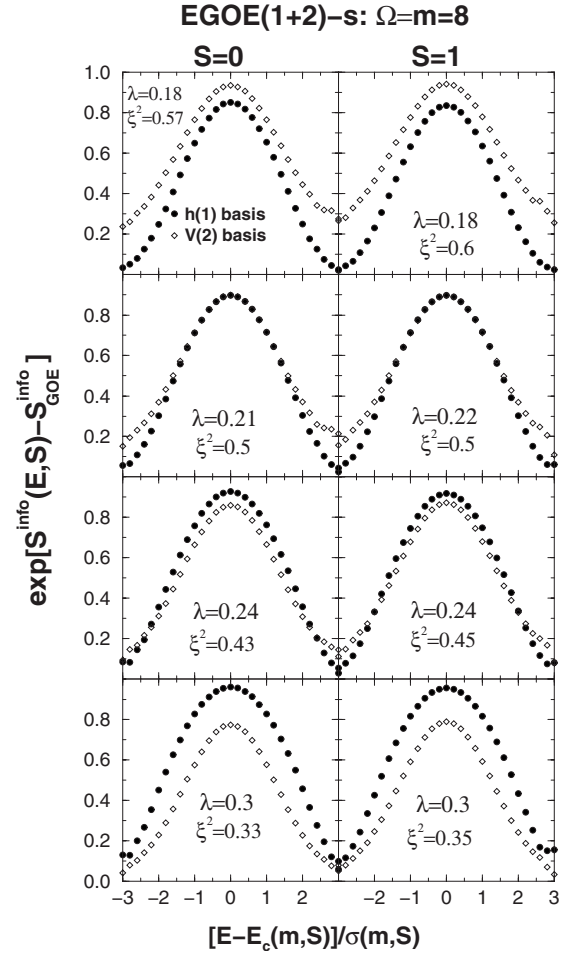


FIG. 7.  $\exp[S^{\text{info}}(E,S) - S_{\text{GOE}}^{\text{info}}]$  in  $h(1)$  and  $V(2)$  basis for a 20 member EGOE(1+2)-s ensemble with  $\Omega=m=8$  and spins  $S=0$  and  $1$  for different  $\lambda$  values. Results averaged over bin size  $0.2$  are shown as circles; filled circles correspond to  $h(1)$  basis and open circles correspond to  $V(2)$  basis. The  $\xi^2$  values defined by Eq. (23b) are also given in the figure. The duality point  $\lambda_d$  corresponds to  $\xi^2=0.5$ . See text for details.

$V(2)$  basis for  $\lambda < \lambda_d$ . The two entropies coincide at  $\lambda = \lambda_d$  and beyond that,  $S^{\text{info}}$  in the  $h(1)$  basis is comparatively larger. For a qualitative understanding of the variation of  $\lambda_d$  with  $S$ , we use the criterion that around the duality region, spreadings produced by  $h(1)$  and  $V(2)$  are equal. This leads to the condition,

$$\sigma_{h(1)}^2(m,S) = \lambda_d^2 P(\Omega, m, S). \quad (24)$$

To determine  $\sigma_{h(1)}^2(m,S)$ , we consider a uniform spectrum with  $\Delta=1$ . This gives,  $\sigma_{h(1)}^2(1, \frac{1}{2}) = (\Omega^2 - 1)/12$ . Then, using Eq. (7),

$$\sigma_{h(1)}^2(m,S) = \mathcal{H}(\Omega, m, S) = \frac{1}{12} [m(\Omega + 2)(\Omega - m/2) - 2\Omega S(S + 1)]. \quad (25)$$

Combining this with Eqs. (13) and (24) will give finally

$$\lambda_d(S) \propto \sqrt{\frac{\mathcal{H}(\Omega, m, S)}{P(\Omega, m, S)}}. \quad (26)$$

Equation (26) with the result  $\lambda_d(S=0)=0.21$  gives  $\lambda_d(S=1)=0.22$  and  $\lambda_d(S=2)=0.24$ . These predictions are close to the numerical results shown in Fig. 7. Therefore Eq. (26) gives a good qualitative understanding of  $\lambda_d(S)$  variation with  $S$ . In the dilute limit, simplifying the  $\mathcal{H}$  and  $P$  factors, we have  $\lambda_d \rightarrow 1/\sqrt{m}$  and this is the result for spinless fermion systems [22]. This also shows that in the dilute limit  $\lambda_d$  and  $\lambda_F$  have same scale. However these scales differ parametrically as  $m$  approaches  $\Omega$  (for  $m > \Omega$  one has to consider holes) and  $S \gtrsim m/4$ . In this situation there is strong spin dependence for the ratio  $\lambda_d/\lambda_F$  as seen from Eqs. (22), (25), and (26) that give  $\lambda_d/\lambda_F \propto \sqrt{\frac{m(\Omega+2)(\Omega-m/2)-2\Omega S(S+1)}{m\Omega^2}}$ . Thus the variance propagator determines the behavior of the three transition markers  $\lambda_c$ ,  $\lambda_F$ , and  $\lambda_d$ .

## VII. OCCUPANCIES, SINGLE-PARTICLE ENTROPY AND THERMODYNAMIC REGION

A very important question for isolated finite interacting particle systems is the following: in the chaotic domain will there be a point or a region where thermalization occurs; i.e., will there be a region where different definitions of entropy, temperature, specific heat, and other thermodynamic variables give the same results (as valid for infinite particle systems) [12,14,40]? Toward answering this question within EGOE(1+2)-s, we consider three different entropies, i.e., thermodynamic entropy defined by the eigenvalue density, information entropy and sp entropy defined by the occupancies of the sp orbitals. Before comparing these three different entropies for various values of  $\lambda$ , now let us first consider occupancies in some detail.

Occupation probability for a sp orbital  $i$  is given by the expectation value of  $n_i$ , i.e.,  $\langle n_i \rangle^{m,S,E}$ . It is possible to write this as a ratio of two densities,

$$\langle n_i \rangle^{m,S,E} = \frac{\langle n_i \delta(H-E) \rangle^{m,S}}{\langle \delta(H-E) \rangle^{m,S}} = \langle n_i \rangle^{m,S} \frac{\rho_{n_i}^{m,S}(E)}{\rho^{m,S}(E)}. \quad (27)$$

As  $n_i$  is a positive-definite operator, the occupancy density  $\rho_{n_i}^{m,S}(E)$  can be represented by a probability density with moments  $M_p(n_i) = \langle n_i H^p \rangle^{m,S} / \langle n_i \rangle^{m,S}$ . The corresponding lower order central moments define Edgeworth corrected Gaussian form for  $\rho_{n_i}^{m,S}(E)$ . For  $\lambda > \lambda_c$ , fluctuations follow GOE and hence  $\langle n_i \rangle^{m,S,E}$  take a smoothed form and they can be written as the ratio of the smoothed forms for the densities in Eq. (27). As the fixed- $(m,S)$  eigenvalue density is Gaussian, the fixed- $(m,S)$  occupancy densities also follow Gaussian form (as discussed ahead, this is verified by calculating the excess parameter). Therefore,

$$\langle n_i \rangle^{m,S,E} \xrightarrow{\lambda \gtrsim \lambda_c} \langle n_i \rangle^{m,S} \frac{\rho_{n_i;G}^{m,S}(E)}{\rho_G^{m,S}(E)}. \quad (28)$$

Figure 8(a) shows occupation numbers for a 200 member EGOE(1+2)-s ensemble with  $\Omega=m=6$  and spin  $S=0$  as a function of  $E$  for various  $\lambda$  values. Results are shown for the

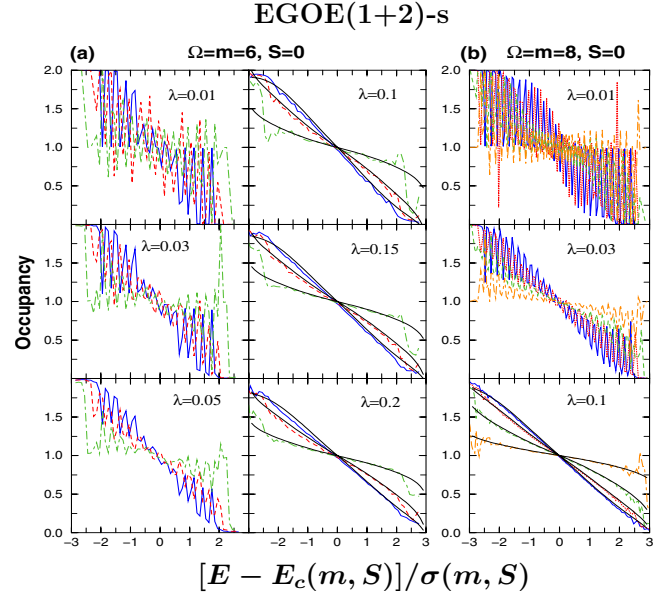


FIG. 8. (Color online) Occupation numbers as a function of  $\hat{E} = [E - E_c(m, S)] / \sigma(m, S)$ . (a) For a 200 member EGOE(1+2)-s ensemble with  $\Omega=m=6$  and spin  $S=0$ , shown are the results for the three lowest sp levels (solid blue, dashed red and dot-dashed green, respectively). They are compared with the EGOE smoothed form (black) given by Eq. (28) for  $\lambda > \lambda_c = 0.05$ . (b) For a 20 member EGOE(1+2)-s ensemble with  $\Omega=m=8$  and spin  $S=0$ , shown are the results for the four lowest sp levels (solid blue, dotted red, dashed green and dot-dashed orange, respectively). They are compared with the EGOE smoothed form (black) given by Eq. (28) for  $\lambda = 0.1$ . For this system,  $\lambda_c = 0.028$ . Note that for the results in the figures, occupancies are averaged over bin size 0.1 for  $\Omega=m=6$  and 0.05 for  $\Omega=m=8$ , respectively. See text for further details.

lowest three sp orbitals. As discussed in Appendix B (see also Fig. 11 ahead),  $\lambda_c = 0.05$  and  $\lambda_F = 0.18$  for the present example. It is clearly seen from Fig. 8(a) that the fluctuations are large for  $\lambda < \lambda_c$  as expected. Beyond this, the occupancies start taking a smoothed form. The numerical results for  $\lambda \gg \lambda_c$  are compared with the smoothed form given by Eq. (28). Here Edgeworth corrections are added to the Gaussian densities. For example, for  $\lambda = 0.1$ , the difference between the occupancy density centroids and the energy centroids (in units of the spectral widths) are  $-0.4$ ,  $-0.29$ , and  $-0.12$  for the sp orbitals 1, 2, and 3, respectively. Similarly the occupancy density widths (in units of the spectral widths) are 0.91, 0.96 and 0.99 and  $\gamma_2$  values are  $-0.39$ ,  $-0.43$  and  $-0.4$  for the sp orbitals 1, 2, and 3, respectively. Note that  $|\gamma_1| \sim 0$  in all the cases. For the eigenvalue density, the excess parameter  $\gamma_2(m, S) = -0.38$ . Agreement between Eq. (28) and the numerical results is excellent except at the spectrum ends as here the states are not sufficiently complex. We have also verified this for  $S=1$  and  $S=2$  examples. Therefore in the  $\lambda < \lambda_c$  region, fluctuations being large (they follow Poisson), smoothed forms are not meaningful. On the other hand, in the chaotic domain defined by  $\lambda > \lambda_c$ , occupation probabilities take a smoothed form as the fluctuations here follow GOE (hence they are small). The smoothed form is well described by Eq. (28). It is interesting to note that the fluctuations even in the ground-state region are small for  $\lambda$

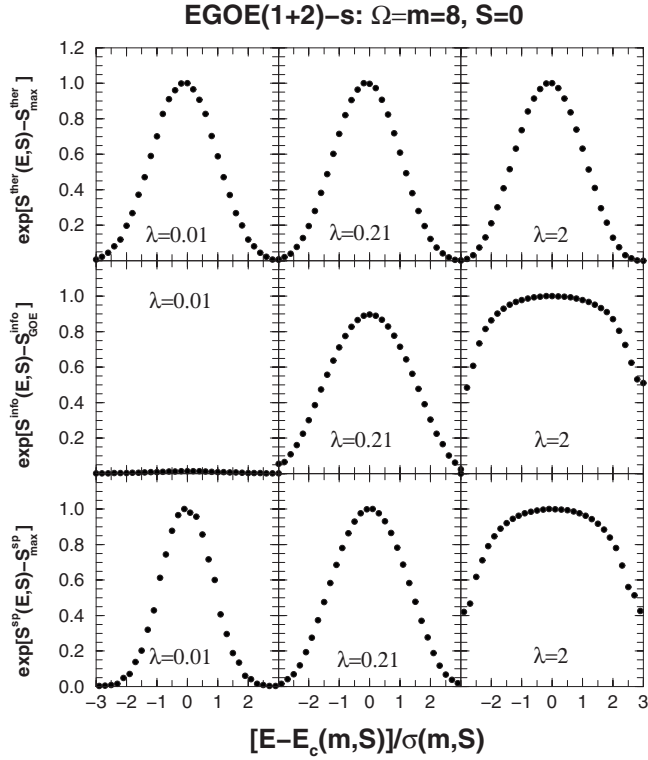


FIG. 9. Thermodynamic entropy  $\exp[S^{ther}(E, S) - S_{max}^{ther}]$ , information entropy  $\exp[S^{info}(E, S) - S_{GOE}^{info}]$  and single-particle entropy  $\exp[S^{sp}(E, S) - S_{max}^{sp}]$  vs  $\hat{E} = [E - E_c(m, S)] / \sigma(m, S)$  for a 20 member EGOE(1+2)-s ensemble with  $\Omega = m = 8$  and  $S = 0$  for different  $\lambda$  values. Entropies averaged over bin size 0.2 are shown as filled circles. Note that for  $\lambda = 0.01$ ,  $\exp[S^{info}(E, S) - S_{GOE}^{info}]$  is close to zero for all  $\hat{E}$  values. See text for details.

$\gg \lambda_F$ . All these conclusions are also verified for a 20 member EGOE(1+2)-s ensemble with  $\Omega = m = 8$  and  $S = 0$  and some of these results are shown in Fig. 8(b).

Given the fractional occupation probabilities  $f_i(E, S) = \frac{1}{2} \langle n_i \rangle^{m, S, E}$ , the sp entropy  $S^{sp}(E, S)$  is defined by

$$S^{sp}(E, S) = - \sum_i 2 \{ f_i(E, S) \ln f_i(E, S) + [1 - f_i(E, S)] \ln [1 - f_i(E, S)] \}. \quad (29)$$

To establish that the  $\lambda = \lambda_d$  region corresponds to the thermodynamic region, we will compare the thermodynamic entropy  $S^{ther}(E) = \ln \rho^{m, S}(E)$  and the information entropy defined by Eqs. (19) and (23a) with the sp entropy for different  $\lambda$  values just as it was done before for EGOE(1+2) and the nuclear shell-model examples [19,20]. For  $\Omega = m = 8$  and  $S = 0$  system with 20 members, we show in Fig. 9 results for  $\lambda = \lambda_d = 0.21$ ,  $\lambda = 0.01 \ll \lambda_d$  and  $\lambda = 2 \gg \lambda_d$ . Note that  $\exp[S^{ther}(E, S) - S_{max}^{ther}] \rightarrow \exp[-\frac{1}{2} \hat{E}^2]$  for all  $\lambda$  values as the eigenvalue density is a Gaussian essentially independent of  $\lambda$ . Similarly, Eq. (23a) gives the formula for  $\exp[S^{info}(E, S) - S_{GOE}^{info}]$ . We have also verified that the extension of the EGOE(1+2) formula for the sp entropy [20] with centroids and variances replaced by fixed- $(m, S)$  centroids and vari-

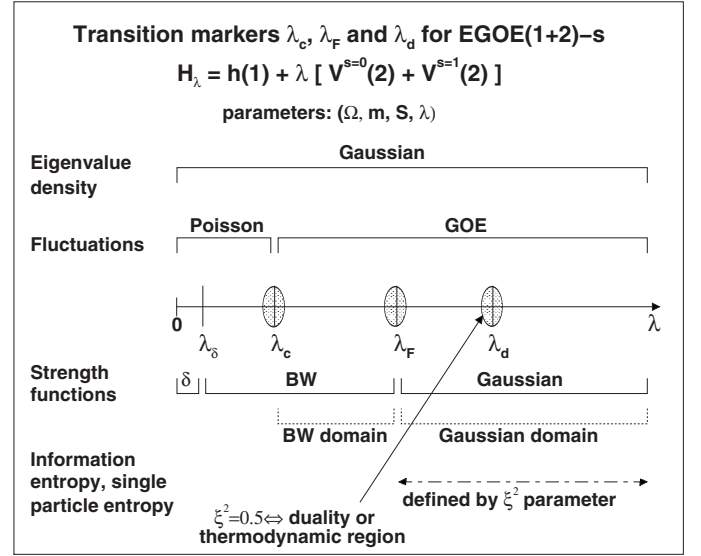


FIG. 10. Transition (chaos) markers for EGOE(1+2)-s. Results in the figure are obtained using the Hamiltonian  $H_\lambda$  given in Eq. (16), i.e.,  $\lambda_0 = \lambda_1 = \lambda$  in Eq. (1). Note that  $\lambda$  is in the units of the average spacing  $\Delta$  of the sp levels defining  $h(1)$ . As discussed in the text, strength functions take  $\delta$ -function form (denoted by  $\delta$  in the figure) for  $\lambda < \lambda_\delta$  with  $\lambda_\delta \ll \lambda_c$  and they start taking BW form as  $\lambda$  crosses  $\lambda_\delta$ . The BW domain is defined by  $\lambda_c < \lambda < \lambda_F$  and here the strength functions take BW form and the fluctuations are GOE. Similarly, in the Gaussian domain, defined by  $\lambda > \lambda_F$ , the strength functions take Gaussian form and the fluctuations are GOE. Also in this region, the information entropy and single-particle entropy are defined by the  $\xi^2$  parameter given in Eq. (23b). The basic structure of the transitions remains same even for  $\lambda_0^2 \neq \lambda_1^2$  as discussed in Appendix B. See text for further details.

ances is a good approximation for fixed- $(E, S)$  sp entropy and then the formula is

$$\exp[S^{sp}(E, S) - S_{max}^{sp}] = \exp - \frac{1}{2} \xi^2 \hat{E}^2. \quad (30)$$

For the three examples shown in Fig. 9,  $\xi^2 = 0.998, 0.5$ , and  $0.039$  for  $\lambda = 0.01, 0.21$ , and  $2$ , respectively. It is clearly seen from Fig. 9 that the three entropies differ as we go away from  $\lambda = \lambda_d$  and at  $\lambda = \lambda_d$  they all look similar, i.e., as stated in [19] “the thermodynamic entropy defined via the global level density or in terms of occupation numbers behaves similar to the information entropy.” Therefore,  $\lambda = \lambda_d$  region can be interpreted as the thermodynamic region in the sense that all different definitions of entropy coincide in this region.

## VIII. CONCLUSIONS

In summary, we have presented in Secs. III–VII, a comprehensive set of calculations for the changes in level fluctuations, strength functions, information entropy and occupancies as a function of the  $\lambda$  parameter in EGOE(1+2)-s Hamiltonian given by Eq. (1) with  $\lambda_0 = \lambda_1 = \lambda$ . The final results are summarized in Fig. 10 (the basic structure of the transitions remains same even for  $\lambda_0^2 \neq \lambda_1^2$  as discussed briefly in Appendix B). In addition, we have derived the

exact formula for the ensemble averaged fixed- $(m, S)$  spectral variances and for the  $V(2)$  part it is of the form  $\lambda^2 P(\Omega, m, S)$ . We have demonstrated that the variance propagator  $P(\Omega, m, S)$  in Eq. (13) gives a good explanation for the spin dependence of the Poisson to GOE and BW to Gaussian crossover points  $\lambda_c$  and  $\lambda_F$  for level fluctuations and strength functions, respectively, and similarly for the duality or thermodynamic region marked by  $\lambda_d$  (obtained from information entropy and occupancies). The three chaos markers  $\lambda_c$ ,  $\lambda_F$  and  $\lambda_d$  in terms of  $P(\Omega, m, S)$  are given by Eqs. (17), (22), and (26), respectively. As seen from Fig. 2,  $P$  decreases with  $S$  and using this in Eqs. (17), (22), and (26), establishes that the  $\lambda_c$ ,  $\lambda_F$  and  $\lambda_d$  values will increase with  $S$  (as  $S=m/2$  corresponds to spinless fermions, it may be possible to investigate further, using EGOE(1+2)-s, the recent claim by Papenbrock and Weidenmüller [56] that symmetries are responsible for chaos in nuclear shell model). Thus, introduction of the spin quantum number preserves the general structures, generated by spinless fermion EGOE(1+2) ensemble, although the actual values of the markers vary with the  $m$ -particle spin  $S$ . It will be interesting and useful to examine in future the energy dependence of the markers  $\lambda_c$ ,  $\lambda_F$ , and  $\lambda_d$ . It should be emphasized that the first example for the transition markers exhibited by EGOE(1+2) with additional good quantum number besides the particle number  $m$  are derived and presented using EGOE(1+2)-s in this paper.

The transition markers as described in Fig. 10 provide a basis for statistical spectroscopy. For example, for  $\lambda \geq \lambda_c$  as GOE fluctuations are small they can be ignored. Then the smoothed eigenvalue densities will be Gaussian. Similarly the strength functions and other related distributions will take BW or Gaussian form. Using these it is possible to derive distributions (with respect to the energy eigenvalues) for various spectroscopic observables [4,12,21,29,34,35] and employ them in applications in nuclear and atomic physics. Moreover if the system is in the thermodynamic region, then Gaussian form can be used for the strength functions (or partial densities) defined over subspaces generated by any symmetry algebra [21,29] and this will allow one to study goodness of group symmetries [47,57]. In a future publication, going beyond strength functions and occupancies, we will consider the distribution of transition strengths generated by a general one-body transition operator that is a vector in the spin space. Transition strengths are observables and they are also useful in many applications [8,35,58,59].

In the present paper, we have presented a detailed analysis of the transition markers using level fluctuation measures nearest-neighbor spacing distribution and  $\Delta_3$  statistic, and occupancies which are often used in spectroscopy. In addition, employed also are the strength functions and information entropy which are used often in quantum chaos studies as delocalization measures. In addition to these traditional measures, it is also possible to employ the new entanglement measures, introduced in the context of QIS, to characterize complexity in quantum many-body systems and for disordered spin-1/2 lattice systems; entanglement and delocalization are found to be strongly correlated [23,60]. As emphasized in [23], this feature may be generic to systems described by two-body ensembles and hence should be investigated in detail. Similarly, in [60] the authors define two-

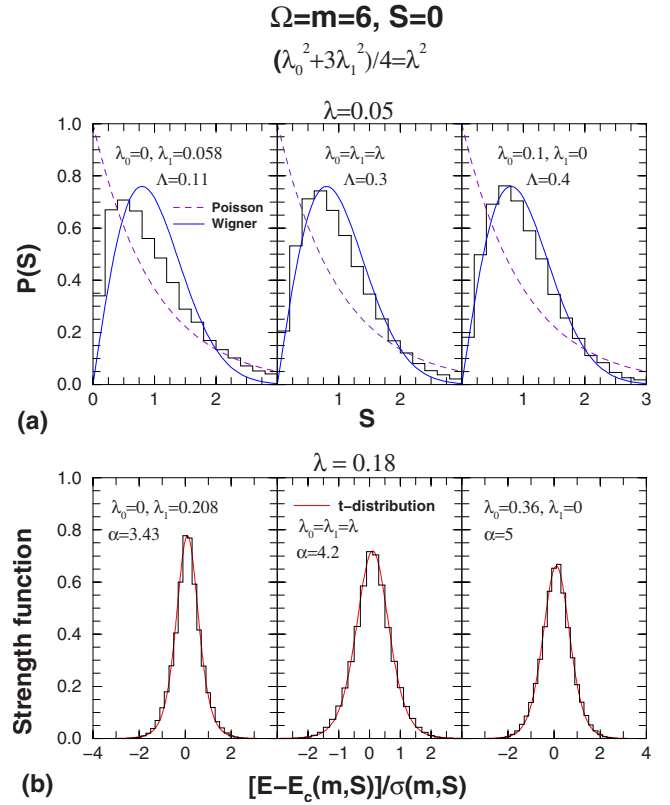


FIG. 11. (Color online) Variation in the nearest-neighbor spacing distributions  $P(S)$  and the strength functions  $F_k(E, S)$  with  $\lambda_0$  and  $\lambda_1$ , for a 200 member EGOE(1+2)-s ensemble with  $\Omega=m=6$  and spin  $S=0$ . Calculations are carried out with the constraint  $(\lambda_0^2 + 3\lambda_1^2)/4 = \lambda^2$  and the results are shown for (a)  $\lambda=0.05$  and (b)  $\lambda=0.18$  with three different values for  $\lambda_0$ . Strength functions are shown for  $\hat{E}_k=0$ . Histograms, with bin size 0.2, are the calculated results. See text for details.

body ensembles for distinguishable quantum particles (spins) and study in particular the distribution of entanglement and quantum correlation measures. Besides the entanglement measures, further analysis of the thermodynamic region generated by two-body ensembles (defined by  $\lambda_d$  in Fig. 10) using long-time averages of various complexity measures as discussed in [40,41] is needed. This, besides being important in QIS, should lead to deeper understanding of wavefunction thermalization in generic isolated many-body quantum systems [40,41,61,62]. These two issues (entanglement and thermalization within EGOE) will be addressed in detail in a future publication.

## ACKNOWLEDGMENTS

Thanks are due to the referees for many useful comments.

## APPENDIX A

Toward providing a basis for the Gaussian form for the eigenvalue density generated by EGOE(1+2)-s, we derive first the exact formula for  $\gamma_2(m, S)$  for a general  $h(1)$  operator and then consider the ensemble averaged  $\gamma_2(m, S)$  for

EGOE(2)-s. Given  $h(1)=\sum_i \epsilon_i n_i$ , the  $\gamma_2(m, S)$  is defined by the fourth central moment  $\langle \tilde{h}^4(1) \rangle^{m, S}$  and the variance or the second central moment  $\langle \tilde{h}^2(1) \rangle^{m, S}$ . Note that

$$\tilde{h}(1) = \sum_{i=1}^{\Omega} \tilde{\epsilon}_i n_i; \quad \tilde{\epsilon}_i = \epsilon_i - \frac{1}{\Omega} \sum_{i=1}^{\Omega} \epsilon_i. \quad (\text{A1})$$

To derive the formula for the fourth moment, we will decompose first  $\tilde{h}^2(1)$  into one and two-body parts. The one-body part of  $\tilde{h}^2(1)$  is defined by the sp energies  $\tilde{\epsilon}_i^2$  and the two-body matrix elements  $V_{ijij}^s = 2\tilde{\epsilon}_i \tilde{\epsilon}_j$  with all other matrix elements being zero; note that  $i \neq j$  for  $s=1$ . Then the  $\lambda$ 's and other averages in Eqs. (9)–(11) are

$$\lambda_{i,i}^{s=0} = -\lambda_{i,i}^{s=1} = 2\tilde{\epsilon}_i^2 - \frac{2}{\Omega} \sqrt{X},$$

$$\langle V(2) \rangle^{2, s} = \frac{2(-1)^s}{\Omega[\Omega + (-1)^s]} \sqrt{X},$$

$$\langle [V(2)]^2 \rangle^{2, s} = \frac{4}{\Omega[\Omega + (-1)^s]} [X + (-1)^s Y],$$

$$\langle [V^{s:\nu=2}(2)]^2 \rangle^{2, s} = \frac{4(-1)^s}{[\Omega + (-1)^s][\Omega + 2(-1)^s]} Y + \frac{4(\Omega^2 + 3(-1)^s \Omega + 3)}{\Omega[\Omega + (-1)^s]^2 [\Omega + 2(-1)^s]} X;$$

$$X = \left( \sum_k \tilde{\epsilon}_k^2 \right)^2, \quad Y = \sum_k \tilde{\epsilon}_k^4. \quad (\text{A2})$$

Using Eq. (8) of [26] with Eqs. (12) and (A2) given above, the final propagation formulas are

$$\langle \tilde{h}^2(1) \rangle^{m, S} = \frac{[m(m-2\Omega)(\Omega+2) + 4\Omega S(S+1)]^2}{4\Omega^2(\Omega^2-1)^2} X,$$

$$\begin{aligned} \langle \tilde{h}^4(1) \rangle^{m, S} &= [\langle \tilde{h}^2(1) \rangle^{m, S}]^2 - \frac{12\mathcal{H}(\Omega, m, S)}{\Omega^2(\Omega^2-1)} (X - \Omega Y) + \frac{[-m(m-2\Omega)\{-4(\Omega+1) + m(\Omega+4)\} + 4\Omega(2\Omega-3m+2)S(S+1)]}{\Omega^2(\Omega+1)(\Omega-1)(\Omega-2)} \\ &\times (X - \Omega Y) + \frac{1}{2\Omega^2(\Omega^2-1)(\Omega-2)^2(\Omega+2)} [m(m-2\Omega)\{-4(\Omega+1) + m(\Omega+4)\}^2 + 8\Omega S(S+1)\{2(\Omega+1)(3\Omega+2) \\ &+ m^2(3\Omega+8) - m(3\Omega^2+16\Omega+12)\} + 16\Omega^2\{S(S+1)\}^2] (X - \Omega Y) + \frac{4}{\Omega^2(\Omega-1)(\Omega+3)} \mathcal{Q}^2(\{2\}; m, S) \\ &\times \langle [V^{s=0:\nu=2}(2)]^2 \rangle^{2, 0} + \frac{4}{\Omega^2(\Omega+1)(\Omega-3)} \mathcal{Q}^2(\{1^2\}; m, S) \langle [V^{s=1:\nu=2}(2)]^2 \rangle^{2, 1}. \end{aligned} \quad (\text{A3})$$

Note that  $\mathcal{H}$  is defined in Eq. (25) and  $\mathcal{Q}$ 's are defined in Eq. (12), respectively. Using Eq. (A3), we can calculate  $\gamma_2(m, S)$  for any set of  $\epsilon_i$ 's and  $(\Omega, m, S)$  where,

$$\gamma_2(m, S) = \frac{\langle \tilde{h}^4(1) \rangle^{m, S}}{[\langle \tilde{h}^2(1) \rangle^{m, S}]^2} - 3. \quad (\text{A4})$$

Expanding the expression, by combining Eqs. (A3) and (A4), for  $\gamma_2(m, S)$  in powers of  $1/\Omega$  and retaining terms upto  $1/\Omega$ , we have

$$\begin{aligned} \gamma_2(m, S) &= \frac{\gamma_2(1, \frac{1}{2})}{m} - \frac{\{m(m-4) + 4S(S+1)\} \{5\gamma_2(1, \frac{1}{2}) + 6\}}{2m^2\Omega} \\ &+ \mathcal{O}\left(\frac{1}{\Omega^2}\right). \end{aligned} \quad (\text{A5})$$

Therefore, for the  $h(1)$  operators with  $|\gamma_2(1)| \sim 1$ , the excess parameter  $\gamma_2(m, S) \rightarrow 0$  for sufficiently large  $m$  and also the spin dependence is weak. Therefore  $h(1)$  operators in general

generate Gaussian eigenvalue densities for large  $m$  values. With  $S=m/2$  and  $N=2\Omega$ , Eq. (A5) reduces to

$$\begin{aligned} \gamma_2(m, S) &= \frac{\gamma_2(1, \frac{1}{2})}{m} + \frac{1}{N} \left[ \frac{\{5\gamma_2(1, \frac{1}{2}) + 6\}}{m} \right. \\ &\left. - \left\{ 5\gamma_2\left(1, \frac{1}{2}\right) + 6 \right\} \right]. \end{aligned} \quad (\text{A6})$$

This is same as the result that follows from the exact formula for  $\gamma_2(N, m)$  for spinless fermion systems [36].

Turning to two-body interactions, first it should be mentioned that a formalism for obtaining exact results for  $\gamma_2(m, S)$  for a given  $V(2)$  is given in [63,64] and also they can be obtained via a subtraction procedure using the formulation discussed in [57]. As seen from [63], the analytical result for  $\gamma_2(m, S)$  is complicated and contains too many terms. Therefore it is not easy to derive an analytical formula for  $\gamma_2(m, S)$  for EGOE(2)-s. However, an analytical understanding is possible in the dilute limit. Then, as argued in

[65], the spin dependence of  $\gamma_2(m, S)$  will be weak and the first correction is of the form  $C_0[1+4S(S+1)/m^2]$  where  $C_0$  is a constant. Strikingly, Eq. (A5), for the  $h(1)$  operator, also gives the same result. Then one can conclude that EGOE(2)-s gives Gaussian eigenvalue densities. In addition, numerical calculations for  $\gamma_2(m, S)$  for EGOE(2)-s, employing the formula derived in [25,66] using the so-called binary correlation approximation, clearly showed [25] that  $|\gamma_2(m, S)|$  will be very small. Combining the analytical results given by Eqs. (A3) and (A5) for  $\gamma_2(m, S)$  for the  $h(1)$  operator and the analytical plus numerical results for EGOE(2)-s, it is plausible to argue that the eigenvalue density for EGOE(1+2)-s will be in general of Gaussian form.

**APPENDIX B**

All the discussion in Secs. IV–VII is restricted to  $\lambda_0=\lambda_1=\lambda$  in Eq. (1), i.e., for equal strengths of the  $s=0$  and  $s=1$  parts of the interaction. However, for completeness, here we present some results for the change in the eigenvalue and wavefunction structure for  $\lambda_0^2 \neq \lambda_1^2$ . To investigate this, we have examined NNSD and strength functions by fixing the value for the ensemble averaged two-particle spectral variance  $\sigma_{V(2)}^2(2)$  generated by the two-body part of  $H$  and then varying  $\lambda_0$  ( $\lambda_1$ ). The two-particle spectral variance for  $\Omega \gg 1$  is  $\sigma_{V(2)}^2(2)=(\lambda_0^2+3\lambda_1^2)/16$ . Therefore we have considered the following Hamiltonian:

$$H_{(\lambda_0, \lambda_1; \lambda)} = h(1) + \lambda_0 V^{s=0}(2) + \lambda_1 V^{s=1}(2); \quad (\lambda_0^2 + 3\lambda_1^2)/4 = \lambda^2, \tag{B1}$$

and carried out calculations for various fixed values of  $\lambda$  and varying  $\lambda_0$  ( $\lambda_1$ ) with the constraint  $(\lambda_0^2+3\lambda_1^2)/4=\lambda^2$ . For a 200 member EGOE(1+2)-s ensemble defined by  $H_{(\lambda_0, \lambda_1; \lambda)}$

with  $\Omega=m=6$  and  $S=0$ , results are presented in Fig. 11 for NNSD and strength functions. In the calculations, we have chosen  $\lambda=0.05$  for NNSD and  $\lambda=0.18$  for the strength functions. For the choice  $\lambda_0=\lambda_1=\lambda$ , they correspond to  $\lambda_c$  and  $\lambda_F$ , respectively, for the  $\Omega=m=6$  and  $S=0$  system. This is clearly seen in Fig. 11. Results are also shown for the two extreme choices  $\lambda_0=0, \lambda_1=\sqrt{4/3}\lambda$  and  $\lambda_0=2\lambda, \lambda_1=0$ . For  $\lambda_0=0$ , the NNSD is closer to Poisson while for  $\lambda_1=0$ , NNSD is much closer to the Wigner form. Similarly, for  $\lambda_0=0$ , the strength function is more closer to BW while for  $\lambda_1=0$ , it is closer to Gaussian. We can easily infer these changes in the structures from the propagator ratio  $R_{(\lambda_0, \lambda_1; \lambda)}(\Omega, m, S) = \sigma_{(\lambda_0, \lambda_1; \lambda)}^2(m, S)/[\lambda^2 P(\Omega, m, S)]$ . Note that  $\sigma_{(\lambda_0, \lambda_1; \lambda)}^2(m, S)$  is same as  $\sigma_{V(2)}^2(m, S)$  given by Eq. (12). For our example with  $\Omega=m=6$  and  $S=0$ , we have  $R_{(\lambda_0, \lambda_1; \lambda)}(\Omega, m, S)=0.93, 0.94, 1, 1.1, 1.22$  for  $\lambda=0.05$  and  $\lambda_0=0, 0.02, 0.05, 0.075$  and  $0.1$ , respectively. Therefore for  $\lambda_0 < 0.05$ , we have  $R_{(\lambda_0, \lambda_1; \lambda)}(\Omega, m, S) < 1$  and this implies [as seen from Eq. (17)] that the level fluctuations change from Poisson-like to GOE as the value of  $\lambda_0$  is increased from  $\lambda_0=0$  as seen in Fig. 11(a). Similarly,  $R_{(\lambda_0, \lambda_1; \lambda)}(\Omega, m, S)=0.93, 0.95, 1, 1.07, 1.22$  for  $\lambda=0.18$  and  $\lambda_0=0, 0.1, 0.18, 0.25$ , and  $0.36$ , respectively. Therefore for  $\lambda_0 < 0.18$ , we have  $R_{(\lambda_0, \lambda_1; \lambda)}(\Omega, m, S) < 1$  and this implies [as seen from Eq. (22)] that the strength functions change from BW to Gaussian form as the value of  $\lambda_0$  is increased from  $\lambda_0=0$  as seen in Fig. 11(b). Thus we can conclude that the general structure of the transitions, as discussed in Fig. 10, remains same even for  $\lambda_0^2 \neq \lambda_1^2$ . We have also made calculations by varying  $\lambda_0$  and  $\lambda_1$  without any constraint. Here also the variance propagator gives predictions for the changes in NNSD and strength functions and we have verified these predictions in some examples.

---

[1] J. B. French and S. S. M. Wong, Phys. Lett. B **33**, 449 (1970); **35**, 5 (1971); O. Bohigas and J. Flores, *ibid.* **34**, 261 (1971); **35**, 383 (1971).  
 [2] K. K. Mon and J. B. French, Ann. Phys. (N.Y.) **95**, 90 (1975).  
 [3] V. K. B. Kota, J. Math. Phys. **46**, 033514 (2005).  
 [4] T. A. Brody, J. Flores, J. B. French, P. A. Mello, A. Pandey, and S. S. M. Wong, Rev. Mod. Phys. **53**, 385 (1981).  
 [5] T. Papenbrock and H. A. Weidenmüller, Rev. Mod. Phys. **79**, 997 (2007).  
 [6] L. Benet, T. Rupp, and H. A. Weidenmüller, Ann. Phys. **292**, 67 (2001).  
 [7] R. J. Leclair, R. U. Haq, V. K. B. Kota, and N. D. Chavda, Phys. Lett. A **372**, 4373 (2008).  
 [8] J. B. French, V. K. B. Kota, A. Pandey, and S. Tomsovic, Ann. Phys. (N.Y.) **181**, 235 (1988).  
 [9] T. Papenbrock and H. A. Weidenmüller, Phys. Rev. C **73**, 014311 (2006).  
 [10] V. K. B. Kota, Int. J. Mod. Phys. E **15**, 1869 (2006).  
 [11] L. Benet and H. A. Weidenmüller, J. Phys. A **36**, 3569 (2003).  
 [12] V. K. B. Kota, Phys. Rep. **347**, 223 (2001).  
 [13] V. V. Flambaum, G. F. Gribakin, and F. M. Izrailev, Phys. Rev. E **53**, 5729 (1996); V. V. Flambaum, F. M. Izrailev, and G. Casati, *ibid.* **54**, 2136 (1996).  
 [14] V. V. Flambaum and F. M. Izrailev, Phys. Rev. E **56**, 5144 (1997).  
 [15] Ph. Jacquod and D. L. Shepelyansky, Phys. Rev. Lett. **79**, 1837 (1997).  
 [16] B. Georgeot and D. L. Shepelyansky, Phys. Rev. Lett. **79**, 4365 (1997).  
 [17] V. K. B. Kota and R. Sahu, Phys. Rev. E **64**, 016219 (2001).  
 [18] Ph. Jacquod and I. A. Varga, Phys. Rev. Lett. **89**, 134101 (2002).  
 [19] M. Horoi, V. Zelevinsky, and B. A. Brown, Phys. Rev. Lett. **74**, 5194 (1995).  
 [20] V. K. B. Kota and R. Sahu, Phys. Rev. E **66**, 037103 (2002).  
 [21] V. K. B. Kota, Ann. Phys. (N.Y.) **306**, 58 (2003).  
 [22] D. Angom, S. Ghosh, and V. K. B. Kota, Phys. Rev. E **70**, 016209 (2004).  
 [23] W. G. Brown, L. F. Santos, D. J. Starling, and L. Viola, Phys. Rev. E **77**, 021106 (2008).  
 [24] V. K. B. Kota, M. Vyas, and K. B. K. Mayya, Int. J. Mod. Phys. E **17**, 318 (2008).

- [25] V. K. B. Kota and K. Kar, Phys. Rev. E **65**, 026130 (2002).
- [26] V. K. B. Kota, N. D. Chavda, and R. Sahu, Phys. Lett. A **359**, 381 (2006).
- [27] H. E. Türeci and Y. Alhassid, Phys. Rev. B **74**, 165333 (2006).
- [28] L. Kaplan, T. Papenbrock, and C. W. Johnson, Phys. Rev. C **63**, 014307 (2000).
- [29] M. Vyas, V. K. B. Kota, and N. D. Chavda, Phys. Lett. A **373**, 1434 (2009).
- [30] Ph. Jacquod and A. D. Stone, Phys. Rev. B **64**, 214416 (2001).
- [31] T. Papenbrock, L. Kaplan, and G. F. Bertsch, Phys. Rev. B **65**, 235120 (2002).
- [32] S. Schmidt and Y. Alhassid, Phys. Rev. Lett. **101**, 207003 (2008).
- [33] J. B. French and V. K. B. Kota, Ann. Rev. Nucl. Part. Sci. **32**, 35 (1982).
- [34] J. Karwowski, Int. J. Quantum Chem. **51**, 425 (1994).
- [35] V. V. Flambaum, A. A. Gribakina, G. F. Gribakin, and I. V. Ponomarev, Physica D **131**, 205 (1999).
- [36] J. B. French, S. Rab, J. F. Smith, R. U. Haq, and V. K. B. Kota, Can. J. Phys. **84**, 677 (2006).
- [37] S. Montangero and L. Viola, Phys. Rev. A **73**, 040302(R) (2006).
- [38] I. Pižorn, T. Prosen, and T. H. Seligman, Phys. Rev. B **76**, 035122 (2007).
- [39] C. Mejía-Monasterio, G. Benenti, G. G. Carlo, and G. Casati, Phys. Rev. A **71**, 062324 (2005).
- [40] M. Rigol, V. Dunjko, and M. Olshanii, Nature (London) **452**, 854 (2008).
- [41] A. C. Cassidy, D. Mason, V. Dunjko, and M. Olshanii, Phys. Rev. Lett. **102**, 025302 (2009).
- [42] J. M. Deutsch, Phys. Rev. A **43**, 2046 (1991).
- [43] M. Srednicki, Phys. Rev. E **50**, 888 (1994).
- [44] Y. Alhassid, Rev. Mod. Phys. **72**, 895 (2000).
- [45] A. Stuart and J. K. Ord, *Kendall's Advanced Theory of Statistics: Distribution Theory* (Oxford University Press, New York, 1987).
- [46] N. D. Chavda, V. Potbhare, and V. K. B. Kota, Phys. Lett. A **311**, 331 (2003).
- [47] J. C. Parikh, *Group Symmetries in Nuclear Structure* (Plenum, New York, 1978).
- [48] C. Quesne, J. Math. Phys. **16**, 2427 (1975).
- [49] K. T. Hecht and J. P. Draayer, Nucl. Phys. A. **223**, 285 (1974).
- [50] V. K. B. Kota, J. Math. Phys. **48**, 053304 (2007).
- [51] L. Muñoz, E. Faleiro, R. A. Molina, A. Relaño, and J. Retamosa, Phys. Rev. E **73**, 036202 (2006).
- [52] O. Bohigas, R. U. Haq, and A. Pandey, in *Nuclear Data for Science and Technology*, edited by K. H. Böckhoff (Reidel, Dordrecht, 1983), p. 809.
- [53] V. K. B. Kota and S. Sumedha, Phys. Rev. E **60**, 3405 (1999).
- [54] T. Guhr and H. A. Weidenmüller, Ann. Phys. **193**, 472 (1989).
- [55] N. D. Chavda, V. Potbhare, and V. K. B. Kota, Phys. Lett. A **326**, 47 (2004).
- [56] T. Papenbrock and H. A. Weidenmüller, Nucl. Phys. A. **757**, 422 (2005).
- [57] S. S. M. Wong, *Nuclear Statistical Spectroscopy* (Oxford University Press, New York, 1986).
- [58] V. K. B. Kota and D. Majumdar, Z. Phys. A **351**, 377 (1995).
- [59] V. V. Flambaum, A. A. Gribakina, G. F. Gribakin, and C. Harabati, Phys. Rev. A **66**, 012713 (2002).
- [60] I. Pižorn, T. Prosen, S. Mossmann, and T. H. Seligman, New J. Phys. **10**, 023020 (2008).
- [61] B. Georgeot and D. L. Shepelyansky, Phys. Rev. E **62**, 6366 (2000).
- [62] V. V. Flambaum, Aust. J. Phys. **53**, 489 (2000).
- [63] J. Karwowski, F. Rajadell, J. Planelles, and V. Mas, At. Data Nucl. Data Tables **61**, 177 (1995).
- [64] J. Planelles, F. Rajadell, J. Karwowski, and V. Mas, Phys. Rep. **267**, 161 (1996).
- [65] J. Planelles, F. Rajadell, and J. Karwowski, J. Phys. A **30**, 2181 (1997).
- [66] S. Tomsovic, Ph.D. thesis, University of Rochester, 1986.